Cancer Letters 275 (2009) 27–34

Contents lists available at ScienceDirect

Cancer Letters

journal homepage: www.elsevier.com/locate/canlet

A novel amplification target, *ARHGAP5*, promotes cell spreading and migration by negatively regulating RhoA in Huh-7 hepatocellular carcinoma cells

Yasuyuki Gen [a], Kohichiroh Yasui [a,*], Keika Zen [a], Tomoaki Nakajima [a], Kazuhiro Tsuji [a], Mio Endo [a], Hironori Mitsuyoshi [a], Masahito Minami [a], Yoshito Itoh [a], Shinji Tanaka [b], Masafumi Taniwaki [c], Shigeki Arii [b], Takeshi Okanoue [a,d], Toshikazu Yoshikawa [a]

[a] *Molecular Gastroenterology and Hepatology, Graduate School of Medical Science, Kyoto Prefectural University of Medicine, 465 Kajii-cho, Kamigyo-ku, Kyoto 602-8566, Japan*
[b] *Department of Hepato-Biliary-Pancreatic Surgery, Tokyo Medical and Dental University, Tokyo, 1-5-45 Yushima, Bunkyo-ku, Tokyo 113-8510, Japan*
[c] *Molecular Hematology and Oncology, Graduate School of Medical Science, Kyoto Prefectural University of Medicine, Kyoto, 465 Kajii-cho, Kamigyo-ku, Kyoto 602-8566, Japan*
[d] *Department of Hepatology, Saiseikai Suita Hospital, Suita, Osaka 564-0013, Japan*

ARTICLE INFO

Article history:
Received 19 August 2008
Received in revised form 23 September 2008
Accepted 30 September 2008

Keywords:
ARHGAP5
p190-B RhoGAP
RhoA
Amplification
Hepatocellular carcinoma

ABSTRACT

RhoA, a member of the Rho family of small GTPases, directs the organization of the actin cytoskeleton and is involved in regulating cell shape and movement. Its activity is negatively regulated by p190-B RhoGAP (GTPase-activating protein). We investigated DNA copy number aberrations in human hepatocellular carcinoma and esophageal squamous cell carcinoma cell lines using a high-density oligonucleotide microarray and found a novel amplification at chromosomal region 14q12. We identified *ARHGAP5* (the gene encoding p190-B RhoGAP) as a probable target for the amplification at 14q12, and our results showed that p190-B RhoGAP promotes cells spreading and migration by negatively regulating RhoA activity in Huh-7 hepatocellular carcinoma cells.

1. Introduction

Members of the Rho family of small GTPases act as molecular switches. In response to extracellular signals, they direct the organization of the actin cytoskeleton and alter gene expression [1]. Rho proteins, which include the much-studied Cdc42, Rac1 and RhoA, are involved in regulating cell shape, polarity and movement and establishing cell-cell junctional complexes. Accordingly, their activity is tightly controlled by regulatory proteins that determine whether GTP or GDP is bound. Rho proteins are activated by guanine nucleotide exchange factors, which catalyze the release of GDP and thus allow GTP to bind the proteins. Rho proteins in turn are inactivated by Rho GTPase-activating proteins (GAPs), which bind to the Rho proteins and induce them to hydrolyze their bound GTP to GDP. p190-B RhoGAP, a member of the RhoGAP family, negatively regulates RhoA activity [2,3].

Amplification of DNA in certain regions of chromosomes plays a crucial role in the development and progression of human malignancies, specifically when proto-oncogenic target genes within those amplicons are overexpressed. Oncogenes that are often amplified in cancers include *MYC*, *ERBB2* and *CCND1*.

In the present study, we investigated DNA copy number aberrations in human hepatocellular carcinoma (HCC) and

* Corresponding author. Tel.: +81 75 251 5519; fax: +81 75 251 0710.
E-mail address: yasuik@koto.kpu-m.ac.jp (K. Yasui).

0304-3835/$ - see front matter © 2008 Elsevier Ireland Ltd. All rights reserved.
doi:10.1016/j.canlet.2008.09.036

esophageal squamous cell carcinoma (ESCC) cell lines and found a novel amplification at chromosomal region 14q12. Because the region may harbor one or more proto-oncogenes whose overexpression following amplification contributes to the initiation or progression of HCC and ESCC, we carried out molecular definition of the amplicon. We show here that the p190-B RhoGAP gene (*ARHGAP5*) within the 14q12 amplicon is amplified and overexpressed, and that p190-B RhoGAP promotes cell spreading and migration in Huh-7 hepatocellular carcinoma cells.

2. Materials and methods

2.1. Cell lines

A total of 10 HCC cell lines (JHH-6, JHH-7, SNU354, SNU398, SNU423, SNU475, Huh-1, Huh-7, HLE and PLC/PRF/5) and 10 ESCC cell lines (T.T, EC-GI-10, KYSE140, KYSE220, TE-4, TE-5, TE-6, TE-10, TE-14 and TE-15) were examined. All cell lines were maintained in Dulbecco's modified Eagle's medium (DMEM) supplemented with 10% fetal calf serum (FCS). Genomic DNA was isolated from each cell line using the Puregene DNA isolation kit (Gentra, Minneapolis, MN, USA).

2.2. Array analysis

Array analyses were performed using the GeneChip Mapping 250K Sty array (Affymetrix, Santa Clara, CA, USA) according to the manufacturer's instructions. In brief, 250 ng of genomic DNA was digested with a restriction enzyme (StyI), ligated to an adaptor and amplified by PCR. Amplified products were fragmented, labeled by biotinylation and hybridized to the microarrays. Hybridization was detected by incubation with streptavidin–phycoerythrin conjugate, and the array was scanned. Analysis was performed as previously described [4]. Copy number changes were calculated using the Copy Number Analyzer for Affymetrix GeneChip Mapping Arrays (CNAG; http://www.genome.umin.jp) [5].

2.3. Fluorescence in situ hybridization (FISH)

We performed FISH using three bacterial artificial chromosomes (BACs), RP11-113E19, RP11-431H16 and RP11-54H22 as probes (Invitrogen, Carlsbad, CA, USA), as described previously [6]. The BACs were selected based on homology with locations in the human genome according to the database provided by the UCSC (http://genome.ucsc.edu/).

2.4. Real-time quantitative PCR

We quantified genomic DNA and mRNA using a real-time fluorescence detection method, as described previously [6]. The primers used were as follows: *ARHGAP5* mRNA (forward, 5′-CATCTGTTTTTGGCCAACCT-3′; reverse, 5′-gtggaggagccacaatgttt-3′); *HEATR5A* mRNA (forward, 5′-TGTGCCTCCTACTCATGCTG-3′; reverse, 5′-gagatggcctgagct tgaac-3′); *c14orf126* mRNA (forward, 5′-gtgctttttcaaggga gctg-3′; reverse, 5′-ttcctccaagggtagcttga-3′); *NUBPL* mRNA (forward, 5′-cttggccttgtccaaaacat-3′; reverse, 5′-acaattggc tggcctgtatc-3′). These primers were designed using Primer3 (http://frodo.wi.mit.edu/cgi-bin/primer3/primer3_www.cgi) based on sequence data obtained from the NCBI database (http://www.ncbi.nlm.nih.gov/). *GAPDH* and long interspersed nuclear element 1 (LINE-1) were used as endogenous controls for mRNA and genomic DNA levels, respectively.

2.5. RNA interference (RNAi)

For RNAi, small interfering RNA (siRNA) duplex oligoribonucleotides targeting *ARHGAP5* (5′-CAAGATCATAATATCAATCTA-3′) and control (non-silencing) siRNA duplexes were synthesized by QIAGEN (Valencia, CA, USA). The siRNAs were delivered into Huh-7 cells using HiPerfect Transfection Reagent (QIAGEN), according to the manufacturer's protocol.

2.6. Immunoblotting

Immunoblots were prepared according to previously reported methods [7]. Cell lysates (20 μg protein per sample) were separated by sodium dodecyl sulfate-polyacrylamide gel electrophoresis on 10% acrylamide gels. Anti-p190-B RhoGAP monoclonal antibody was obtained from BD Transduction Laboratories (Lexington, KY, USA); anti-RhoA monoclonal antibody was from Santa Cruz Biotechnology (Santa Cruz, CA, USA); and anti-β-actin monoclonal antibody was from Sigma–Aldrich (Tokyo, Japan). For immunoblotting, we used anti-p190-B RhoGAP, anti-RhoA and anti-β-actin at dilutions of 1:250, 1:100 and 1:5000, respectively. For secondary immunodetection, we used anti-mouse IgG (Amersham, Tokyo, Japan) diluted 1:5000. Protein binding was detected using the ECL system (Amersham).

2.7. RhoA activity assay

Active RhoA levels were measured using the enzyme-linked immunosorbent assay (ELISA)-based G-LISA RhoA activation assay Biochem Kit (Cytoskeleton, Denver, CO, USA) according to the manufacturer's instructions. In brief, Huh-7 cells were transfected with siRNA targeting *ARHGAP5* or negative control siRNA, or were left untreated. Cells were then cultured under the standard conditions in DMEM containing 10% FCS. After 48 h, cells were harvested for the RhoA activity assay or trypsinized and held in suspension for 1 h in DMEM containing 1% FCS. The suspended cells were then plated on 6-well plates coated with 5 μg/ml fibronectin (BD Transduction Laboratories) and harvested for the RhoA activity assay at the indicated time points. For the RhoA activity assay, cells were lysed in 70 μl of G-LISA lysis buffer, scraped into tubes and snap frozen in liquid nitrogen. Cell lysates were subsequently thawed, clarified for 2 min at 10,000g, and protein concentrations were normalized between the various time points. Equal amounts of total protein were added to a 96-well plate coated with the Rho-binding domain of Rho effector pro-

teins (which bind active GTP-bound Rho) in triplicate and incubated at 4 °C for 30 min with vigorous shaking. Active Rho levels were determined by subsequent incubations with anti-Rho antibody and secondary horseradish peroxidase-conjugated antibody for 45 min each at room temperature. After adding developing solution, the level of active Rho was determined by measuring absorbance at 490 nm using an ELISA plate reader. Equal loading of total RhoA protein at each time point was determined via immunoblotting using anti-RhoA antibody as described above. Experiments were repeated at least three times.

2.8. Immunofluorescence

Huh-7 cells were transfected with siRNA targeting *ARHGAP5* or negative control siRNA or were left untreated. Cells were harvested 48 h after transfection, suspended for 1 h in DMEM containing 1% FCS and then plated on glass slides coated with fibronectin for 10, 20, 40, 60 or 180 min. Cells were fixed for 10 min in 3.7% formaldehyde, permeabilized for 2 min in 1% Triton X-100 and incubated for 1 h with a blocking buffer (phosphate-buffered saline containing 3% bovine serum albumin). The cells were then incubated for 1 h at room temperature with anti-p190-B RhoGAP monoclonal antibody diluted 1:200 in blocking buffer. Fluorescein isothiocyanate (FITC)-conjugated anti-mouse IgG (Cappel, Aurora, OH, USA) was used to detect the primary antibody. Actin filaments and nuclei were counterstained with rhodamine-phalloidin (Molecular Probes, Eugene, OR, USA) and 4',6-diamidino-2-phenylindole (DAPI; Sigma–Aldrich), respectively.

2.9. Monolayer wound healing assay

Huh-7 cells were transfected with siRNA targeting *ARHGAP5* or negative control siRNA or left untreated. After 24 h, cells in DMEM with 1% FCS were seeded on glass slides coated with fibronectin and allowed to adhere overnight.

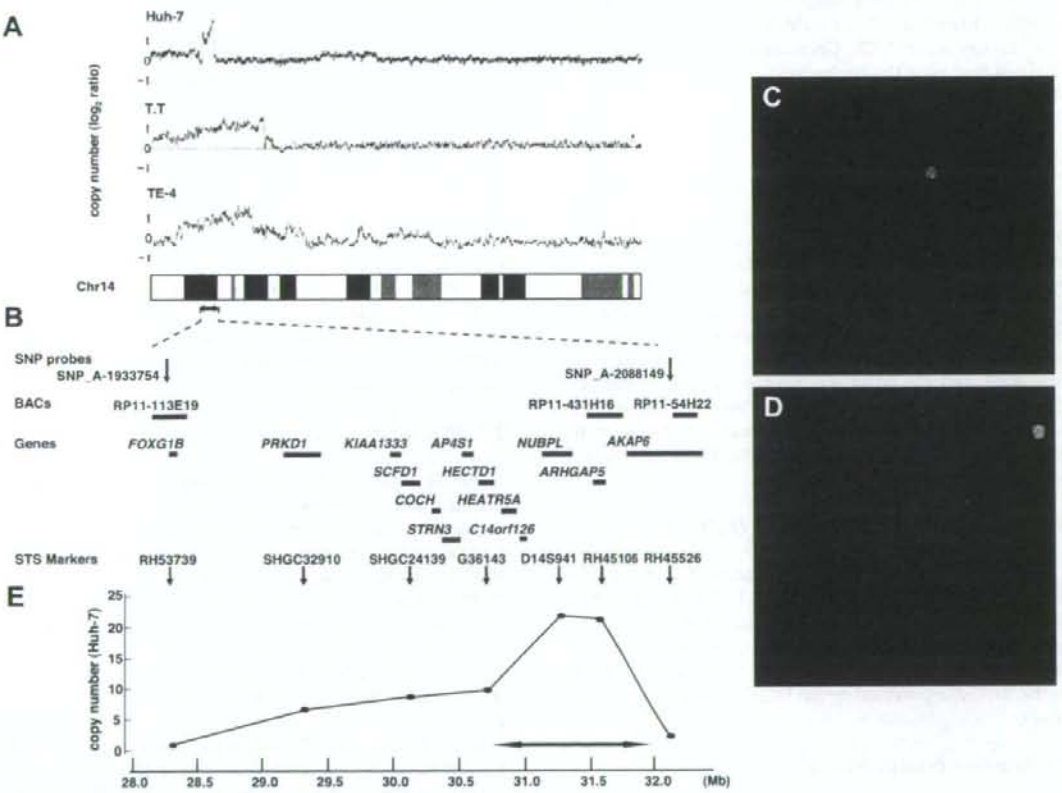

Fig. 1. Map of the amplicon at 14q12. (A) Copy number profiles for chromosome 14 in Huh-7, T.T and TE-4 cells. Copy number values were determined by GeneChip Mapping 250 K array analyses. (B) The positions of the Affymetrix SNP probes, three BACs used as probes for FISH experiments, the 13 genes within the 14q12 amplicon, and the seven STS markers used for real-time quantitative PCR on genomic DNA are shown according to the UCSC genome database (http://genome.ucsc.edu/). (C and D) Representative images of two-color FISH on metaphase chromosomes from Huh-7 cells using BACs: paired RP11-431H16 (green; C) and RP11-113E19 (red; C), or paired RP11-431H16 (green; D) and RP11-54H22 (red; D). (E) Copy numbers at the seven STS marker loci in Huh-7 cells as measured by real-time quantitative PCR with reference to LINE-1 controls. Values are normalized such that the copy number in genomic DNA derived from normal lymphocytes has a value of 2. The smallest region of amplification is indicated (arrow).

We scratched wounds in the cell monolayer using a sterile 200-μl pipet tip, rinsed the cells with phosphate-buffered saline and added DMEM containing 10% FCS with or without mitomycin C (10 μg/ml, Nacalai Tesque, Kyoto, Japan). Cells were allowed to migrate into the wound for 0, 12, or 24 h before fixation. Cells were stained with Giemsa stain (Nacalai Tesque) or were triple-labeled with anti-p190-B RhoGAP, rhodamine-phalloidin and DAPI as described above. Wound widths were measured in three randomly chosen regions. Experiments were repeated at least three times.

2.10. Statistical analysis

Analysis of variance (ANOVA) was performed using SPSS 15.0 software (SPSS Inc., Chicago, IL, USA). *P* values of <0.05 were considered significant.

3. Results

3.1. Detection of 14q12 amplicon in HCC and ESCC cell lines by array analyses

We screened for DNA copy number aberrations in 10 HCC cell lines and 10 ESCC cell lines using GeneChip Mapping 250 K array analysis. Of the 20 cell lines, one HCC cell line, Huh-7, and two ESCC cell lines, T.T and TE-4, commonly exhibited copy number gains at chromosomal region 14q12 (Fig. 1A). In particular, Huh-7 cells showed a high-level gain indicative of amplification in a narrow region on 14q12 between the positions recognized by the Affymetrix SNP_A-1933754 and SNP_A-2088149 probes. To confirm amplification in Huh-7 cells, we performed FISH analyses using BACs RP11-113E19, RP11-431H16 and RP11-54H22 as probes (Fig. 1B–D). BAC RP11-431H16 generated strong signals as a small homogeneously staining region (HSR), indicating amplification (Figs. 1C, D). In contrast, BACs RP11-113E19 or RP11-54H22 did not show a HSR pattern, indicating their positions outside the amplicon (Fig. 1C and D). Furthermore, we determined gene dosages in Huh-7 cells at the STS markers RH53739, SHGC32910, SHGC24139, G36143, D14S941, RH45106, and RH45526 loci by real time quantitative PCR. (Fig.1B and E). The highest copy number was observed at the D14S941 and RH45106 loci. Taken together, we defined the smallest region of amplification between markers G36143 and RH45526. The extent of the amplicon was estimated to be 1.2 Mb. This region includes four known or predicted protein-coding genes, *HEATR5A*, *c14orf126*, *NUBPL*, and *ARHGAP5*.

3.2. Identification of candidate target genes in the 14q12 amplicon

The 14q12 region may harbor one or more genes (henceforth called 'target genes') that, when activated by amplification, play a role in carcinogenesis. A common criterion for designating a gene as a putative target is that amplification leads to its overexpression [8]. Using real-time quantitative PCR, we determined mRNA levels of all four genes within the amplicon in the 10 HCC cell lines and 10 ESCC cell lines. Among the four genes, *HEATR5A* and *ARHGAP5* were commonly overexpressed in Huh-7, T.T and TE-4 cells, the cell lines that were found to have copy number gains at 14q12 (Fig. 2A). These findings identified *ARHGAP5*, which encodes p190-B RhoGAP, as one of candidate target genes for the 14q12 amplicon.

We determined copy numbers of *ARHGAP5* in the 10 HCC and 10 ESCC cell lines by real-time quantitative PCR (Fig. 2B). Copy number changes were counted as gains if the results of the analysis for a given tumor cell type exceeded the twofold levels of the gene in normal cells. A copy number gain of *ARHGAP5* was observed in six (30%) of the 20 cell lines: Huh-7, T.T, KYSE140, TE-4, TE-6 and TE-10.

We examined the expression of p190-B RhoGAP protein in 4 HCC and 4 ESCC cell lines by immunoblot analysis. As shown in Fig. 2C, expression levels of p190-B RhoGAP were higher in cell lines exhibiting copy number gains of *ARHGAP5* (Huh-7, T.T, KYSE140, TE-4 and TE-10) than other cell lines that did not show gains (SNU354, Huh-1 and PLC/PRF/5).

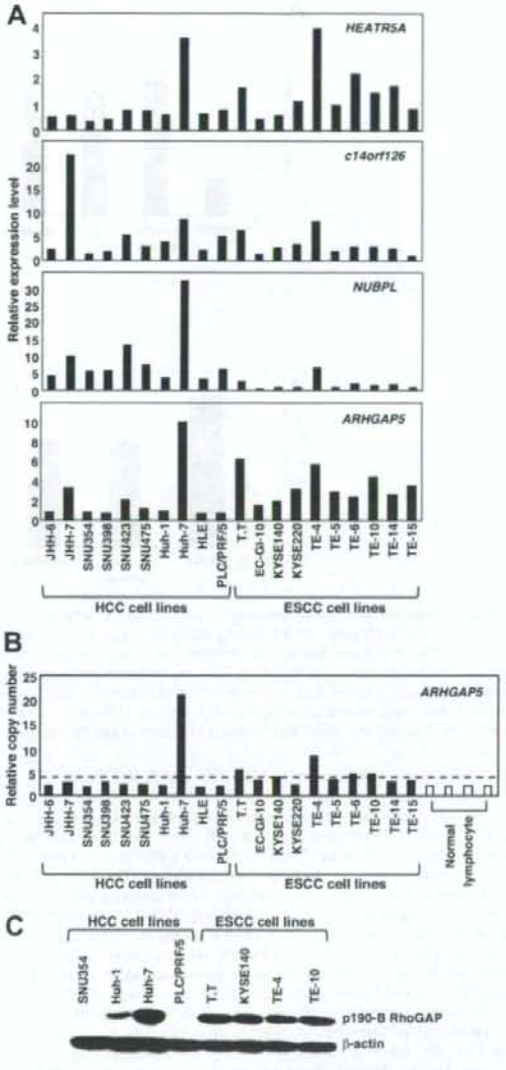

Fig. 2. Amplification and overexpression of *ARHGAP5* in Huh-7, T.T and TE-4 cell lines. (A) Relative expression levels of four genes (*HEATR5A*, *c14orf126*, *NUBPL* and *ARHGAP5*) within the 14q12 amplicon in 10 HCC and 10 ESCC cell lines as evaluated by real-time quantitative PCR. Results are presented as expression levels of each gene relative to a reference gene (*GAPDH*) to correct for variations in the amount of RNA. (B) Copy numbers at the *ARHGAP5* locus (the STS marker RH45106) in 10 HCC cell lines, 10 ESCC cell lines and four normal peripheral blood lymphocytes as measured by real-time quantitative PCR with reference to LINE-1 controls. Values are normalized such that the average copy number in genomic DNA derived from four normal lymphocytes has a value of 2. A value of 4, which is a twofold increase in copy number of normal lymphocytes, was used to determine the cut-off value for copy number gain, shown as a dotted line. (C) Levels of p190-B RhoGAP and β-actin, an internal control, determined by immunoblotting in 4 HCC and 4 ESCC cell lines.

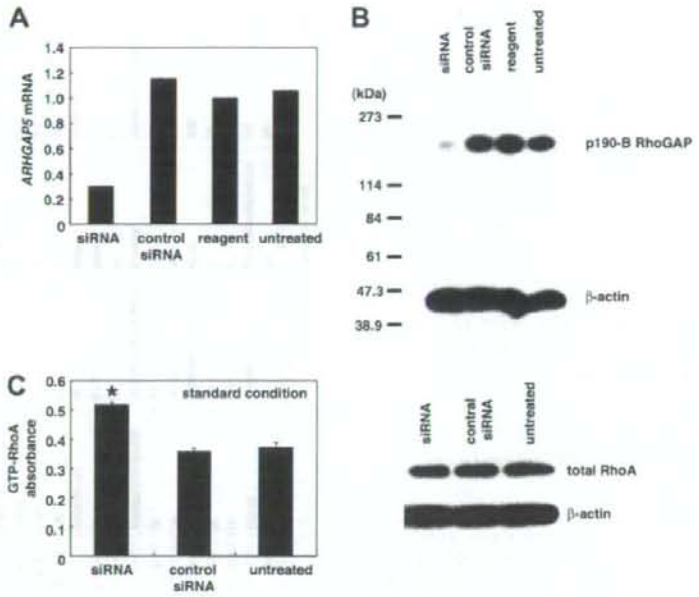

Fig. 3. Knockdown of *ARHGAP5* increases RhoA activity. (A) Relative expression levels of *ARHGAP5* mRNA as determined by real-time quantitative PCR. Huh-7 cells were treated with siRNA targeting *ARHGAP5*, negative control siRNA or transfection agent alone. Untreated cells were maintained under identical experimental conditions. Results are presented as a ratio between the expression level of *ARHGAP5* and that of a reference gene (*GAPDH*) to correct for variation in the amount of RNA. Relative expression levels were normalized such that the ratio in untreated cells was 1. (B) Levels of p190-B RhoGAP and β-actin, an internal control, determined by immunoblotting. (C) (*left*) Levels of RhoA activity under standard culture conditions (DMEM containing 10% FCS). RhoA activity was measured using a G-LISA kit (see Methods section). Values are represented as the mean ± S.D. Differences were analyzed by ANOVA ($^{*}P < 0.05$). (*right*) Total RhoA and β-actin were determined by immunoblotting.

3.3. Regulation of RhoA activity by p190-B RhoGAP in Huh-7 cells

To investigate the biological function of p190-B RhoGAP in HCC cells, knockdown of *ARHGAP5* expression in Huh-7 cells was carried out using RNAi. Following treatment of Huh-7 cells with siRNA targeting *ARHGAP5*, we observed a decrease in both *ARHGAP5* mRNA and p190-B RhoGAP protein levels relative to what was observed for cells receiving control siRNA, transfection agent alone or left untreated (Fig. 3A and B). Because p190-B RhoGAP negatively regulates RhoA activity, we examined the effect of the siRNA-mediated knockdown of *ARHGAP5* on RhoA activity. Huh-7 cells were treated with *ARHGAP5* siRNA or control siRNA or were left untreated. Cells were then cultured in DMEM containing 10% FCS for 48 h under standard conditions. RhoA activity levels were higher in cells treated with *ARHGAP5* siRNA than in cells treated with control siRNA or in untreated cells, whereas total RhoA levels were similar among the three groups (Fig. 3C). These findings suggest that overexpression of *ARHGAP5* contributes to downregulation of RhoA activity in Huh-7 cells.

3.4. Regulation of cell spreading by p190-B RhoGAP in Huh-7 cells

It is known that integrin-mediated adhesion regulates the activity of p190-B RhoGAP and RhoA [3,9]. We therefore examined the function of p190-B RhoGAP when Huh-7 cells were plated on fibronectin, a specific ligand for α5β1 integrin. Huh-7 cells treated with *ARHGAP5* siRNA or control siRNA or left untreated were suspended and plated on fibronectin. Prior to and during plating, cells were maintained in DMEM containing 1% FCS. Adhesion to fibronectin regulated RhoA activity in a triphasic or biphasic manner (Fig. 4A). Prior to plating (0 min), RhoA activity was significantly higher in *ARHGAP5* siRNA-treated cells than in control siRNA-treated cells or untreated cells. In *ARHGAP5* siRNA-treated cells, RhoA activity rapidly and transiently decreased (20 min). This initial decline was followed by an increase that peaked at 60 min. In the final phase, RhoA activity gradually decreased. In control siRNA-treated cells or untreated cells, an initial period of low RhoA activity was followed by a slight increase that peaked between 40–60 min and then returned to basal level. RhoA activity was significantly higher in *ARHGAP5* siRNA-treated cells than control siRNA-treated cells or untreated cells between 40 and 180 min. During the experimental period, expression of p190-B RhoGAP was continuously knocked down by *ARHGAP5* siRNA and total RhoA levels were similar among the three groups (Fig. 4A).

Because RhoA affects cell motility by stimulating reorganization of actin, we examined whether p190-B RhoGAP regulates the spreading of Huh-7 cells on fibronectin. Using immunofluorescence, we observed morphological changes in Huh-7 cells during attachment and spreading on fibronectin (Fig. 4B). Phalloidin staining revealed that *ARHGAP5* siRNA-treated cells exhibited more robust actin stress fibers but less membrane ruffling and protrusion at the cell periphery than control siRNA-treated cells or untreated cells. The actin stress fiber formation and reduced membrane ruffling and protrusion observed in *ARHGAP5* siRNA-treated cells corresponded with higher RhoA activity (Fig. 4)

p190-B RhoGAP was expressed diffusely in the cytoplasm of control siRNA-treated cells and untreated cells, whereas it was hardly detected in *ARHGAP5* siRNA-treated cells. We found that p190-B RhoGAP had partially translocated to the membrane protrusions in control siRNA-treated cells and untreated cells by 40 min after plating (Fig. 4B). Taken together, these findings suggest that RhoA inactivation by p190-B RhoGAP results in inhibition of actin stress fiber formation, enhanced membrane ruffling and protrusion and promotion of cell spreading on fibronectin.

3.5. Regulation of cell migration by p190-B RhoGAP in Huh-7 cells

To investigate the role of p190-B RhoGAP in cell motility, we performed a monolayer wound healing assay. Wound closure was delayed in *ARHGAP5* siRNA-treated cells relative to control siRNA-treated cells or untreated cells, whether cultured in the presence of mitomycin C or in its absence (Figs. 5A–E). Mitomycin C blocks mitosis and thus allows analysis of cell migration in the absence of cell proliferation. These results show that cell migration, rather than cell proliferation, is the major factor

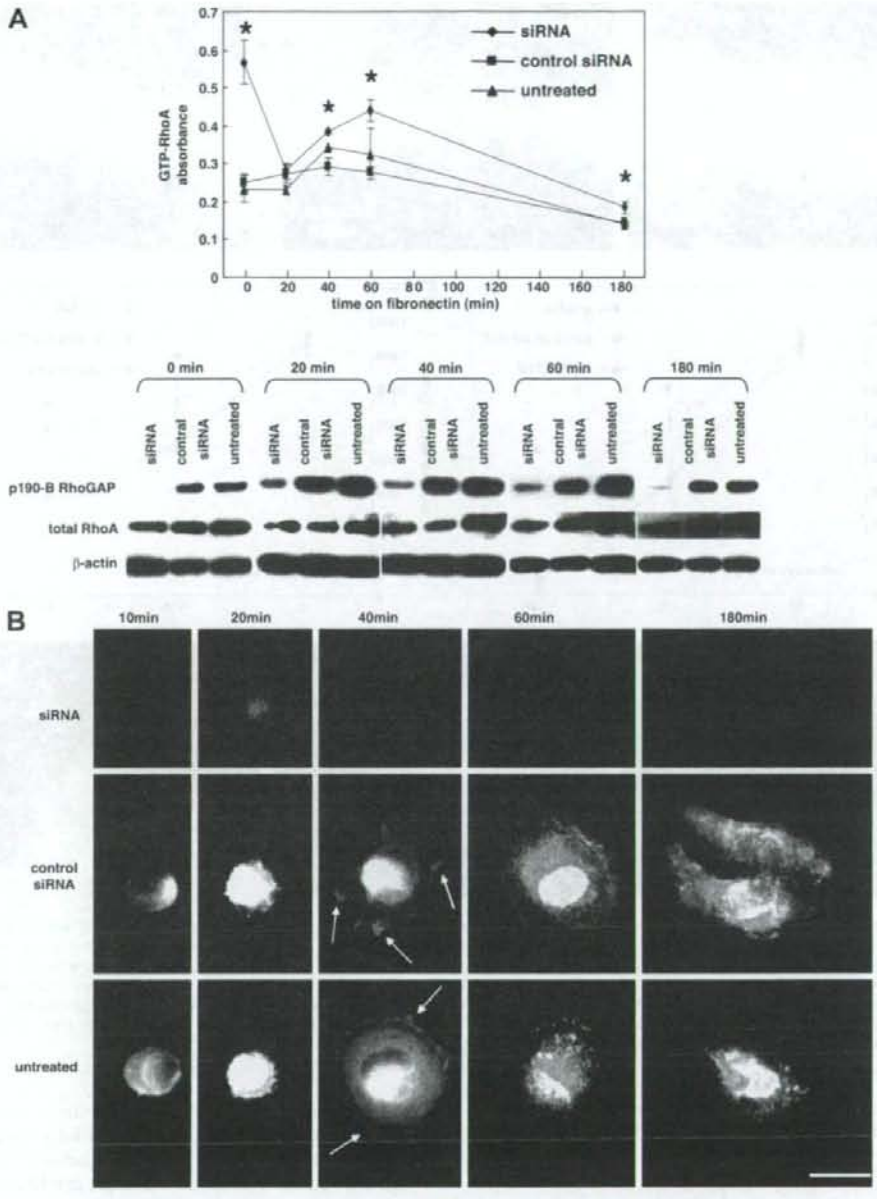

Fig. 4. Knockdown of *ARHGAP5* inhibits Huh-7 cell spreading on fibronectin. (A) Time course of changes in RhoA activity (*upper*) and levels of p190-B RhoGAP and total RhoA (*lower*). Huh-7 cells treated with siRNA targeting *ARHGAP5* or control siRNA or left untreated were plated on fibronectin as described in Materials and Methods and harvested at the indicated time points. Values of RhoA activity are represented as the mean ± SD. Differences were analyzed by ANOVA ($^{*}P < 0.05$). Levels of p190-B RhoGAP, total RhoA and β-actin were determined by immunoblotting. (B) Time course of cell spreading on fibronectin. Huh-7 cells treated with siRNA targeting *ARHGAP5* or control siRNA or left untreated were plated on fibronectin, fixed at the indicated time points and then triple-labeled with anti-p190-B RhoGAP, rhodamine-conjugated phalloidin and DAPI to reveal p190-B RhoGAP (green), actin filaments (red), and nuclei (blue), respectively. Arrows indicate p190-B RhoGAP on membrane protrusions. Scale bar = 10 μm.

in the retarded wound repair process in *ARHGAP5* siRNA-treated cells. Wound edge cells in *ARHGAP5* siRNA-treated cells had more abundant actin stress fibers but less membrane ruffling and protrusion at the leading edge than control siRNA-treated or untreated cells (Figs. 5F–H). p190-B RhoGAP translocated to the membrane protrusions of control siRNA-treated or untreated cells at the edge of the wound, but not in *ARHGAP5*-siR-

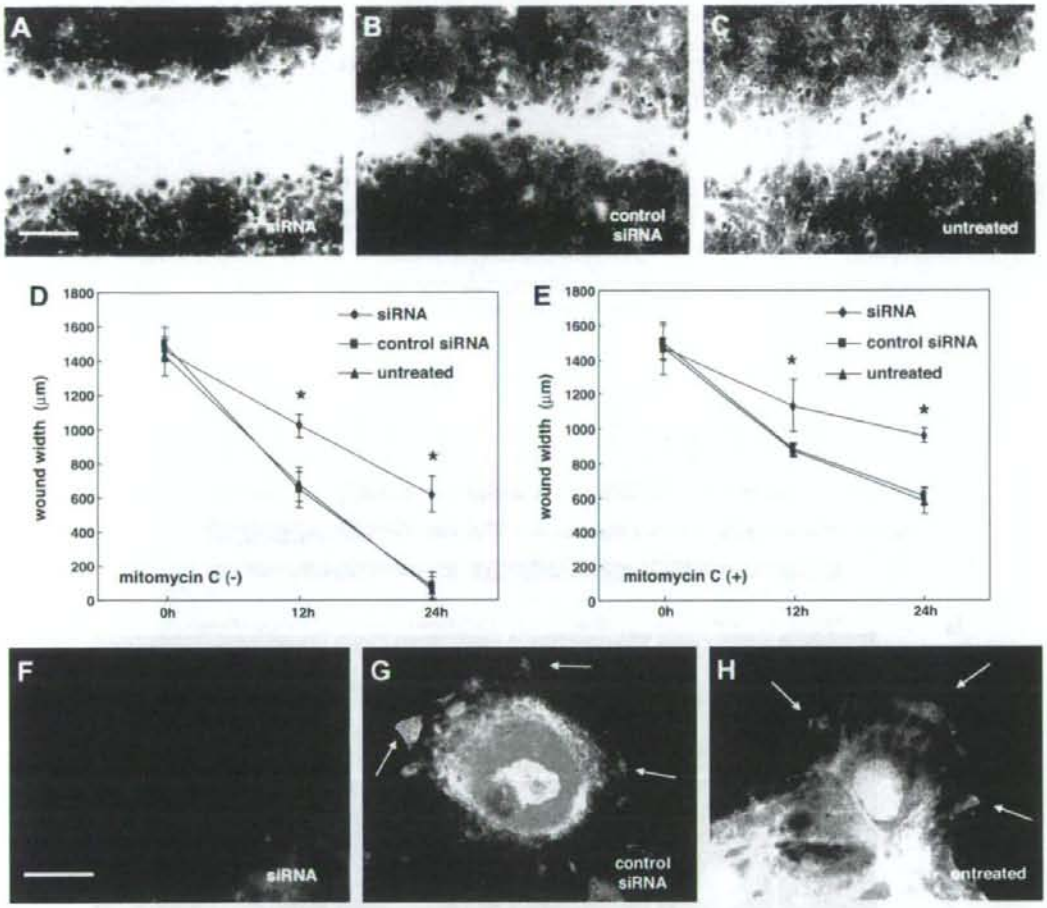

Fig. 5. Knockdown of *ARHGAP5* inhibits migration in Huh-7 cells. Monolayer wound healing assay in Huh-7 cells transfected with siRNA targeting *ARHGAP5* (A, F) or control siRNA (B and G), or left untreated (C and H). Cells were cultured in the absence (A–D, F–H) or presence (E) of mitomycin C. (A–C) Cells were allowed to migrate into a monolayer wound for 24 h and afterward stained with Giemsa stain. Original magnifications: 40×. Scale bar = 500 μm. (D and E) Cells were cultured in the absence (D) or presence (E) of mitomycin C. Wound widths were measured in three randomly chosen regions at the indicated time after wounding. Values are represented as the mean ± SD. Differences were analyzed by ANOVA (*$P < 0.05$). (F–H) Wound edge cells were triple-labeled with anti-p190-B RhoGAP, rhodamine-conjugated phalloidin and DAPI to reveal p190-B RhoGAP (green), actin filaments (red) and nuclei (blue), respectively. Arrows indicate p190-B RhoGAP on membrane protrusions. Scale bar = 10 μm.

NA cells. Taken together, these observations suggest that the inhibition of RhoA activity by p190-B RhoGAP promotes cell movement and formation of membrane protrusions in migrating cells.

4. Discussion

We report here the amplification of *ARHGAP5* in HCC and ESCC cell lines. We undertook a molecular definition of the amplicon at 14q12 that is present in HCC and ESCC cell lines. The amplification at 14q12 has been reported in various types of cancers, including HCC [10], ESCC [7], nasopharyngeal carcinoma [11] and non-squamous cell lung carcinoma [12], although the frequency of 14q12 gain is low in primary HCC (4–6%) [10,13]. The range of the amplicon varies among these tumors, and their boundaries have not been determined in each case. Moreover, the target oncogene(s) in the amplified regions have not been fully identified. Here we defined the amplified regions in one HCC and two ESCC cell lines and narrowed the site of the amplification to a relatively short section. Among the four genes within the smallest region of the amplification, only *HEATR5A* and *ARHGAP5* were overexpressed in all the tested lines exhibiting copy number gains in the region; hence they are thought to be candidate targets in the amplicon. Of the two genes, we chose to focus further analysis on *ARHGAP5* because its protein product, p190-B RhoGAP, is purported to play an important role in dynamic cellular processes by regulating RhoA activity, while little is known about *HEATR5A*. During the preparation of this manuscript, amplification of *ARHGAP5* was reported in Huh-7 cells [14].

Although several studies have suggested an association of p190-B RhoGAP with tumors [15–17], its biological function in cancer cells is poorly understood. Therefore, using siRNA, we studied its function in Huh-7 cells, the HCC cell line that exhibited the most remarkable copy number gain and overexpression of *ARHGAP5*. We found that p190-B RhoGAP negatively regulates RhoA activity in Huh-7 cells cultured in medium containing 10% FCS and plated on fibronectin. Adhesion to fibronectin regulated RhoA activity in a triphasic or biphasic manner, as previously reported in fibroblasts [18,19]. Although some RhoA activity is required for migration, possibly to maintain sufficient adhesion to the substrate, high activity inhibits movement [19–22]. Our results showed that RhoA inactivation by p190-B RhoGAP results in inhibition of actin stress fiber formation, enhanced membrane ruffling and protrusion, and promotion of spreading and migration of Huh-7 cells. These findings are in agreement with results obtained from previous studies. A dominant negative (loss-of-function) p190-B RhoGAP mutation elevates RhoA activity in fibroblasts cultured on fibronectin and inhibits their migration, whereas overexpression of wild-type p190-B RhoGAP decreases RhoA activity, promotes the formation of membrane protrusions and enhances mobility [19]. Activation of β1 integrin signaling stimulates tyrosine phosphorylation of p190-B RhoGAP and promotes membrane protrusion at invadopodia in a melanoma cell line [17]. p190-B RhoGAP is also involved in invasion by breast cancer cells [15].

In conclusion, we have identified *ARHGAP5* as a probable target for the amplification at 14q12 detected in a subgroup of HCCs and ESCCs. Our results indicate that p190-B RhoGAP, the protein product of *ARHGAP5*, promotes cell spreading and migration in Huh-7 cells. Further studies are needed to determine the importance of *ARHGAP5* and p190-B RhoGAP in the development and progression of not only HCC and ESCC but also other types of tumors.

Conflicts of interest statement

My co-authors and I declare that we have no proprietary, financial, professional or other personal interest of any nature or kind in any product, service and/or company that could be construed as influencing the position presented in the manuscript entitled, "A novel amplification target, ARHGAP5, promotes cell spreading and migration by negatively regulating RhoA in Huh-7 hepatocellular carcinoma cells".

Acknowledgements

Supported by: Grants-in-Aid for Scientific Research (18390223) from the Japan Society for the Program of Science (to K.Yasui).

References

[1] A. Hall, Rho GTPases and the actin cytoskeleton, Science 279 (1998) 509–514.
[2] P.D. Burbelo, S. Miyamoto, A. Utani, S. Brill, K.M. Yamada, A. Hall, Y. Yamada, P190-B, a new member of the Rho GAP family, and Rho are induced to cluster after integrin cross-linking, J. Biol. Chem. 270 (1995) 30919–30926.
[3] W.T. Arthur, L.A. Petch, K. Burridge, Integrin engagement suppresses RhoA activity via a c-Src-dependent mechanism, Curr. Biol. 10 (2000) 719–722.
[4] G.C. Kennedy, H. Matsuzaki, S. Dong, W.N. Liu, J. Huang, G. Liu, X. Su, M. Cao, W. Chen, J. Zhang, W. Liu, G. Yang, X. Di, T. Ryder, Z. He, U. Surti, M.S. Phillips, M.T. Boyce-Jacino, S.P. Fodor, K.W. Jones, Large-scale genotyping of complex DNA, Nat. Biotechnol. 21 (2003) 1233–1237.
[5] Y. Nannya, M. Sanada, K. Nakazaki, N. Hosoya, L. Wang, A. Hangaishi, M. Kurokawa, S. Chiba, D.K. Bailey, G.C. Kennedy, S. Ogawa, A robust algorithm for copy number detection using high-density oligonucleotide single nucleotide polymorphism genotyping arrays, Cancer Res. 65 (2005) 6071–6079.
[6] Y. Inagaki, K. Yasui, M. Endo, T. Nakajima, K. Zen, K. Tsuji, M. Minami, S. Tanaka, M. Taniwaki, Y. Itoh, S. Arii, T. Okanoue, CREB3L4, INTS3, and SNAPAP are targets for the 1q21 amplicon frequently detected in hepatocellular carcinoma, Cancer Genet. Cytogenet. 180 (2008) 30–36.
[7] K. Yasui, I. Imoto, Y. Fukuda, A. Pimkhaokham, Z.Q. Yang, T. Naruto, Y. Shimada, Y. Nakamura, J. Inazawa, Identification of target genes within an amplicon at 14q12–q13 in esophageal squamous cell carcinoma, Genes Chromosomes Cancer 32 (2001) 112–118.
[8] C. Collins, J.M. Rommens, D. Kowbel, T. Godfrey, M. Tanner, S.I. Hwang, D. Polikoff, G. Nonet, J. Cochran, K. Myambo, K.E. Jay, J. Froula, T. Cloutier, W.L. Kuo, P. Yaswen, S. Dairkee, J. Giovanola, G.B. Hutchinson, J. Isola, O.P. Kallioniemi, M. Palazzolo, C. Martin, C. Ericsson, D. Pinkel, D. Albertson, W.B. Li, J.W. Gray, Positional cloning of ZNF217 and NABC1: genes amplified at 20q13.2 and overexpressed in breast carcinoma, Proc. Natl. Acad. Sci. USA 95 (1998) 8703–8708.
[9] E.A. Cox, S.K. Sastry, A. Huttenlocher, Integrin-mediated adhesion regulates cell polarity and membrane protrusion through the Rho family of GTPases, Mol. Biol. Cell 12 (2001) 265–277.
[10] C. Śakakura, A. Hagiwara, H. Taniguchi, T. Yamaguchi, H. Yamagishi, T. Takahashi, K. Koyama, Y. Nakamura, T. Abe, J. Inazawa, Chromosomal aberrations in human hepatocellular carcinomas associated with hepatitis C virus infection detected by comparative genomic hybridization, Br. J. Cancer 80 (1999) 2034–2039.
[11] Y.J. Chen, J.Y. Ko, P.J. Chen, C.H. Shu, M.T. Hsu, S.F. Tsai, C.H. Lin, Chromosomal aberrations in nasopharyngeal carcinoma analyzed by comparative genomic hybridization, Genes Chromosomes Cancer 25 (1999) 169–175.
[12] T. Yakut, H.J. Schulten, A. Demir, D. Frank, B. Danner, U. Egeli, C. Gebitekin, E. Kahler, B. Gunawan, N. Urer, H. Oztürk, L. Füzesi, Assessment of molecular events in squamous and non-squamous cell lung carcinoma, Lung Cancer 54 (2006) 293–301.
[13] P. Moinzadeh, K. Breuhahn, H. Stützer, P. Schirmacher, Chromosome alterations in human hepatocellular carcinomas correlate with aetiology and histological grade – results of an explorative CGH meta-analysis, Br. J. Cancer 92 (2005) 935–941.
[14] C. Schlaeger, T. Longerich, C. Schiller, P. Bewerunge, A. Mehrabi, G. Toedt, J. Kleeff, V. Ehemann, R. Eils, P. Lichter, P. Schirmacher, B. Radlwimmer, Etiology-dependent molecular mechanisms in human hepatocarcinogenesis, Hepatology 47 (2008) 511–520.
[15] S. Zrihan-Licht, Y. Fu, J. Settleman, K. Schinkmann, L. Shaw, I. Keydar, S. Avraham, H. Avraham, RAFTK/Pyk2 tyrosine kinase mediates the association of p190 RhoGAP with RasGAP and is involved in breast cancer cell invasion, Oncogene 19 (2000) 1318–1328.
[16] G. Chakravarty, D. Roy, M. Gonzales, J. Gay, A. Contreras, J.M. Rosen, P190-B, a Rho-GTPase-activating protein, is differentially expressed in terminal end buds and breast cancer, Cell Growth Differ. 11 (2000) 343–354.
[17] H. Nakahara, S.C. Mueller, M. Nomizu, Y. Yamada, Y. Yeh, W.T. Chen, Activation of beta1 integrin signaling stimulates tyrosine phosphorylation of p190RhoGAP and membrane-protrusive activities at invadopodia, J. Biol. Chem. 273 (1998) 9–12.
[18] X.D. Ren, W.B. Kiosses, M.A. Schwartz, Regulation of the small GTP-binding protein Rho by cell adhesion and the cytoskeleton, EMBO J. 18 (1999) 578–585.
[19] W.T. Arthur, K. Burridge, RhoA inactivation by p190RhoGAP regulates cell spreading and migration by promoting membrane protrusion and polarity, Mol. Biol. Cell 12 (2001) 2711–2720.
[20] K. Takaishi, T. Sasaki, M. Kato, W. Yamochi, S. Kuroda, T. Nakamura, M. Takeichi, Y. Takai, Involvement of Rho p21 small GTP-binding protein and its regulator in the HGF-induced cell motility, Oncogene 9 (1994) 273–279.
[21] A.J. Ridley, P.M. Comoglio, A. Hall, Regulation of scatter factor/hepatocyte growth factor responses by Ras, Rac, and Rho in MDCK cells, Mol. Cell. Biol. 15 (1995) 1110–1122.
[22] C.D. Nobes, A. Hall, Rho GTPases control polarity, protrusion, and adhesion during cell movement, J. Cell Biol. 144 (1999) 1235–1244.

 doi: 10.1111/j.1872-034X.2008.00464.x

Original Article

Analysis of hepatic genes involved in the metabolism of fatty acids and iron in nonalcoholic fatty liver disease

Hironori Mitsuyoshi[1], Kohichiroh Yasui[1], Yuichi Harano[2], Mio Endo[1], Kazuhiro Tsuji[1], Masahito Minami[1], Yoshito Itoh[1], Takeshi Okanoue[3] and Toshikazu Yoshikawa[1]

[1]*Molecular Gastroenterology and Hepatology, Graduate School of Medical Science, Kyoto Prefectural University of Medicine, Kyoto,* [2]*Department of Hepatology, Akashi City Hospital, Akashi,* [3]*Saiseikai Suita Hospital, Suita, Japan*

Aims: Hepatic steatosis and iron cause oxidative stress, thereby progressing steatosis to steatohepatitis. We quantified the expression of genes involved in the metabolism of fatty acids and iron in patients with nonalcoholic fatty liver disease (NAFLD).

Methods: The levels of transcripts for the following genes were quantified from biopsy specimens of 74 patients with NAFLD: thioredoxin (Trx), fatty acid transport protein 5 (FATP5), sterol regulatory element-binding protein 1c (SREBP1c), fatty acid synthase (FASN), acetyl-coenzyme A carboxylase (ACAC), peroxisome proliferative activated receptor α (PPARα), cytochrome P-450 2E1 (CYP2E1), acyl-coenzyme A dehydrogenase (ACADM), acyl-coenzyme A oxidase (ACOX), microsomal triglyceride transfer protein (MTP), transferrin receptor 1 (TfR1), transferrin receptor 2 (TfR2) and hepcidin. Twelve samples of human liver RNA were used as controls. Histological evaluation followed the methods of Brunt.

Results: The levels of all genes were significantly higher in the NAFLD patients than in controls. The Trx level increased as the stage progressed. The levels of FATP5, SREBP1c, ACAC, PPARα, CYP2E1, ACADM and MTP significantly decreased as the stage and grade progressed ($P < 0.05$). Hepatic iron score (HIS) increased as the stage progressed. The TfR1 level significantly increased as the stage progressed ($P < 0.05$), whereas TfR2 level significantly decreased ($P < 0.05$). The ratio of hepcidin mRNA/ferritin ($P < 0.001$) or hepcidin mRNA/HIS ($P < 0.01$) was significantly lower in NASH patients than simple steatosis patients.

Conclusions: Steatosis-related metabolism is attenuated as NAFLD progresses, whereas iron-related metabolism is exacerbated. Appropriate therapies should be considered on the basis of metabolic changes.

Key words: fatty acids, iron, NAFLD, oxidative stress

Abbreviations
Trx, thioredoxin; FATP5, fatty acid transport protein 5; SREBP1c, sterol regulatory element-binding protein 1c; FASN, fatty acid synthase; ACAC, acetyl-coenzyme A carboxylase; PPARα, peroxisome proliferative activated receptor α; CYP2E1, cytochrome P-450 2E1; ACADM, acyl-coenzyme A dehydrogenase; ACOX, acyl-coenzyme A oxidase; MTP, microsomal triglyceride transfer protein; TfR1, transferrin receptor 1; TfR2, transferrin receptor 2.

INTRODUCTION

NON ALCOHOLIC FATTY liver disease (NAFLD) is a wide-spectrum liver disease, ranging from simple steatosis to steatohepatitis.[1] Owing to the obesity epidemic, NAFLD is now recognized as a leading health problem worldwide.[1] Since NAFLD has been documented to progress to liver failure[2] and/or hepatocellular carcinoma,[3] various therapeutic studies for NAFLD or nonalcoholic steatohepatitis (NASH) have been conducted to date.[4–8] These studies included weight reduction,[4] use of insulin sensitizers,[5] antioxidants,[6] phlebotomy[7] and hepato-protective drugs,[8] albeit with limited success. Although these treatments are aimed at addressing the pathogenesis of NAFLD, they would not always be efficient at every stage of this "wide spectrum" disease.

NASH is thought to develop through a "two-hit theory".[9] The first hit includes insulin resistance, mostly due to obesity.[9] The second hits include oxidative stress, inflammatory cytokines, and bacterial endotoxin.[9] In particular, the accumulation of fatty acids in the liver results in oxidative stress through oxidation of fatty

Correspondence: Dr Hironori Mitsuyoshi, Molecular Gastroenterology and Hepatology, Graduate School of Medical Science, Kyoto Prefectural University of Medicine, Kawaramachi Hirokoji, Kamigyo-ku, Kyoto 602-8566, Japan. Email: hmitsu@koto.kpu-m.ac.jp
Received 22 July 2008; revised 22 September 2008; accepted 1 October 2008.

acids.[10] In addition, hepatic iron load, which also induces oxidative stress, has been reported in some groups of patients with NAFLD.[11] Therefore, hepatic metabolism of fatty acids and iron should be the therapeutic target for NAFLD. However, their roles in the development of NAFLD have not yet been studied

In this study, we quantified the expression of genes involved in hepatic metabolism of fatty acids and iron using liver biopsy specimens from patients with NAFLD, and compared them with liver histology. Based on the results, we explored the role of the metabolism of fatty acids and iron in NAFLD. Our study should improve out understanding of the pathogenesis of NAFLD and contribute to the identification of putative therapeutic pathways.

PATIENTS AND METHODS

Patients

NAFLD PATIENTS WHO underwent liver biopsies in our institute between April 2000 and March 2007 were retrospectively selected according to the following criteria: no excessive alcohol intake (more than 20 g/day), as assessed by interview (on at least three occasions); no history of treatment with steatosis-inducing drugs within the 12 months prior to the study; negative serum hepatitis C virus (HCV) antibody; negative for hepatitis B surface antigen or antibodies to human immunodeficiency virus; and an absence of other forms of chronic liver disease, such as autoimmune liver diseases. Anthropometry and laboratory data were collected from all patients at the time of the liver biopsy. All patients had given written informed consent for the analysis of metabolic genes and liver biopsies before the study. The study protocol conformed to the ethical guidelines of the 1975 Declaration of Helsinki and was approved by the Ethics Committee of the Kyoto Prefectural University of Medicine.

Laboratory determinations

After a 12-h overnight fast, venous blood samples were drawn to determine asparatate aminotransferase (AST), alanine aminotransferase (ALT), albumin, total cholesterol, triglyceride, fasting plasma glucose (FPG), glycosylated haemoglobin (HbA_{1c}), insulin and ferritin levels. These parameters were measured using standard techniques from clinical chemistry laboratories. The index of insulin resistance was calculated only in patients without overt diabetes (fasting plasma glucose >126 mg/dL), according to the homeostasis model assessment (HOMA).

Histological evaluation

Formalin-fixed and paraffin-embedded liver biopsy specimens were stained with hematoxylin–eosin, Masson's trichrome, and Perl's Prussian blue. The stage of hepatic fibrosis was scored according to Brunt[12]: 1, zone 3 fibrosis; 2, zone 3 fibrosis with periportal fibrosis; 3, bridging fibrosis; and 4, cirrhosis. The grade of inflammation was scored as follows[12]: 1, mild; 2, moderate; and 3, severe. We considered the scores of stage and grade of simple steatosis as "0". Steatosis was assessed according to the percentage of hepatocytes containing fat droplets. The degree of iron loading was graded using a Perl's score of 0–4, as described previously.[13]

Quantification of the expression of hepatic genes

Liver specimens were immediately frozen after the biopsy and were stored at −80°C until use. Total RNA was isolated from biopsy specimens using the RNeasy kit (Qiagen, Hilden, Germany). First-strand cDNA was obtained from total RNA using the QuantiTect Reverse Transcription kit (Qiagen). PCR was performed using the Light Cycler 2.0 System (Roche, Mannheim, Germany), and the mRNA levels were normalized to those of β-actin. Comprehensive target genes were as follows: thioredoxin (Trx), fatty acid transport protein 5 (FATP5), sterol regulatory element-binding protein 1c (SREBP1c), fatty acid synthase (FASN), acetyl-coenzyme A carboxylase (ACAC), peroxisome proliferative activated receptor α (PPARα), cytochrome P-450 2E1 (CYP2E1), acyl-coenzyme A dehydrogenase, C4 to C12 straight chain (ACADM), acyl-coenzyme A oxidase (ACOX), microsomal triglyceride transfer protein (MTP), transferrin receptor 1 (TfR1), transferrin receptor 2 (TfR2) and hepcidin. Table 1 summarizes the specific primers for these target genes. Twelve samples of human total liver RNA were obtained from commercial sources (Stratagene, CA, USA; Clontech Laboratories, CA, USA; Ambion, TX, USA; Becton, Dickinson, NJ, USA; Cell Applications, CA, USA), and used as controls.

Statistical analysis

Associations between variables were analyzed using the Spearman's correlation coefficient by rank. Differences between variables were analyzed using the Mann–Whitney U-test or Kruskal–Wallis test. All analyses were performed using SPSS software for Windows, version

Table 1 The specific primers used for the target genes

	Sense primers	Antisense primers
Trx	5′-CTGCTTTTCAGGAAGCCTTG-3′	5′-ACCCACCTTTTGTCCCTTCT-3′
FATP5	5′-ACACACTCGGTGTCCCTTTC-3′	5′-CTACAGGGCCCACTGTCATT-3′
SREBP1c	5′-TGCATTTTCTGACACGCTTC-3′	5′-CCAAGCTGTACAGGCTCTCC-3′
FASN	5′-TTCCGAGATTCCATCCTACG-3′	5′-TGTCATCAAAGGTGCTCTCG-3′
ACAC	5′-GAGAACTGCCCTTTCTGCAC-3′	5′-CCAAGCTCCAGGCTTCATAG-3′
PPARα	5′-GGAAAGCCCACTCTGCCCCCT-3′	5′-AGTCACCGAGGAGGGGCTCGA-3′
CYP2E1	5′-CCCAAAGGATATCGACCTCA-3′	5′-AGGGTGTCCTCCACACACTC-3′
ACADM	5′-TTGAGTTCACCGAACAGCAG-3′	5′-AGGGGGACTGGATATTCACC-3′
ACOX	5′-TGATGCGAATGAGTTTCTGC-3′	5′-AGTGCCACAGCTGAGAGGTT-3′
MTP	5′-CATCTGGCGACCCTATCAGT-3′	5′-GGCCAGCTTTCACAAAAGAG-3′
TfR1	5′-ATGCATTTTGCAGCAGTGAG-3′	5′-TCCAAAAGGCCCTACTCCTT-3′
TfR2	5′-GACCCTGCAGTGGGTGTACT-3′	5′-CAGTCGCTCGTCTCTCTCCT-3′
hepcidin	5′-ACCAGAGCAAGCTCAAGACC-3′	5′-AAACAGAGCCACTGGTCAGG-3′

Note: The role of genes analyzed in lipid and iron metabolisms is as follows: oxidative stress-induced, Trx; uptake of fatty acid, FATP5; synthesis of fatty acid, SREBP1c, FASN, ACAC; oxidation of fatty acid, PPARα, CYP2E1, ACADM, ACOX; secretion of triglyceride, MTP; uptake of transferrin-bound iron, TfR1, TfR2; regulation of iron metabolism, hepcidin.
Trx, thioredoxin; FATP5, fatty acid transport protein 5; SREBP1c, sterol regulatory element-binding protein 1c; FASN, fatty acid synthase; ACAC, acetyl-coenzyme A carboxylase; PPARα, peroxisome proliferative activated receptor α; CYP2E1, cytochrome P-450 2E1; ACADM, acyl-coenzyme A dehydrogenase; ACOX, acyl-coenzyme A oxidase; MTP, microsomal triglyceride transfer protein; TfR1, transferrin receptor 1; TfR2, transferrin receptor 2.

14.0 (SPSS, Chicago, IL, USA). A P value of less than 0.05 was considered significant.

RESULTS

The characteristics of patients

TABLES 2 AND 3 summarize the characteristics of patients and the results of liver histology, respectively. Of the 16 diabetic patients, 3 had been treated with metformin, 2 with pioglitazone, 2 with sulfonylurea, and the others had been followed with diet restriction. Serum triglyceride levels were greater in the simple steatosis patients than in the NASH patients. Although the values of HbA_{1c} were comparable in the two groups, those of HOMA-IR [index of insulin resistance (IR)] were significantly higher in the NASH

Table 2 Patients characteristics

	Simple steatosis ($n = 33$)	NASH ($n = 41$)	P value
Age	55.4 ± 15.0	61.2 ± 12.7	0.051
BMI (kg /m^2)	27.5 ± 2.4	26.5 ± 4.4	0.748
Sex (male/female)	24/9	25/16	0.208
Diabetes (yes/no)	7/26	9/32	0.584
Plt	21.6 ± 3.9	19.1 ± 6.3	0.006
AST	43.0 ± 21.4	72.9 ± 30.5	0.0002
ALT	62.3 ± 30.8	89.8 ± 50.3	0.006
Alb	4.7 ± 0.3	4.6 ± 0.3	0.023
T-Cho	231.1 ± 50.5	199.9 ± 44.0	0.006
TG	205.0 ± 105.8	140.9 ± 103.2	0.015
FPG	145.1 ± 68.4	116.7 ± 21.5	0.356
HbA_{1c}	6.6 ± 1.8	6.0 ± 0.6	0.533
HOMA-IR	2.9 ± 1.2	4.6 ± 1.8	0.012
ferritin	223.1 ± 106.0	197.7 ± 160.7	0.227

Note: The value is expressed as either mean ± S.D. or the number of patients.
ALT, alanine aminotransferase; AST, asparatate aminotransferase; Alb, albumin; BMI, body mass index; FPG, fasting plasma glucose; HbA_{1c}, glycosylated haemoglobin; HOMA-IR, homeostasis model assessment-index of insulin resistance; T-Cho, total cholesterol; TG, triglyceride.

Table 3 Results of liver biopsy

	Simple steatosis	NASH
Stage: 1/2/3/4		13/13/13/2
Grade: 1/2/3		27/10/4
Iron: 0/1/2/3	11/12/3/1	14/8/6/6
Steatosis:		
<30%	14	18
30%–60%	7	13
60% <	2	10

NASH, nonalcoholic steatohepatitis.

patients than in the simple steatosis patients. Neither significant fibrosis nor inflammation was observed in the biopsy specimens from patients with simple steatosis. Six specimens from simple steatosis patients and seven specimens from NASH patients were not available for iron staining.

Hepatic oxidative stress

We evaluated hepatic oxidative stress by the level of hepatic Trx, since Trx is known to be a redox-sensitive molecule.[14] We have previously reported that serum Trx levels are a marker of NASH.[15] We measured hepatic thioredoxin mRNA, because it would reflect the redox status of the liver more precisely than serum thioredoxin levels. Hepatic thioredoxin consists of both reduced and oxidized forms, whereas serum thioredoxin is an oxidized form. Therefore, hepatic thioredoxin levels do not correlate with serum thioredoxin levels. The Trx level increased in the order of controls, then simple steatosis patients with the highest levels in NASH patients (Table 4). The differences among the groups were significant (Table 4). The Trx level tended to increase as the stage progressed; however, it did not show any association with the grade (Table 5).

Fatty acid metabolism

The levels of transcripts for the genes involved in fatty acid metabolism were increased in the order of controls, then NASH patients with the highest levels in simple steatosis patients (Table 4). The differences among the groups were significant (Table 4). When values were compared between simple steatosis and NASH patients by the Mann–Whitney's test, the difference was significant in FATP5 ($P < 0.01$), ACAC ($P < 0.05$), PPARα ($P < 0.05$), CYP2E1 ($P < 0.05$), ACADM ($P < 0.05$), ACOX ($P < 0.05$), MTP ($P < 0.05$). Levels of all these genes were significantly higher in the simple steatosis patients than the NASH patients. When compared with the liver histology, the levels of FATP5, SREBP1c, ACAC, PPARα, CYP2E1, ACADM and MTP significantly decreased as the stage and grade progressed (Table 5). The level of ACOX tended to decrease as the stage and grade progressed (Table 5). The level of FASN was similarly decreased, although the difference between groups

Table 4 The levels of hepatic gene involved in lipid and iron metabolism

	Control	Simple steatosis	NASH	*P* value
Trx	1.0 ± 1.1	2.3 ± 0.9	2.5 ± 1.0	$P < 0.00001$
FATP5	1.0 ± 0.4	6.1 ± 3.6	4.3 ± 2.5	$P < 0.00001$
SREBP1c	1.0 ± 0.6	73.9 ± 74.3	56.0 ± 85.4	$P < 0.00001$
FASN	1.0 ± 1.0	28.2 ± 26.8	17.8 ± 15.1	$P < 0.00001$
ACAC	1.0 ± 0.8	12.2 ± 5.9	8.7 ± 3.4	$P < 0.00001$
PPARα	1.0 ± 0.8	21.1 ± 11.3	15.5 ± 8.1	$P < 0.00001$
CYP2E1	1.0 ± 0.4	8.0 ± 4.2	6.2 ± 3.2	$P < 0.00001$
ACADM	1.0 ± 0.9	17.8 ± 9.7	13.1 ± 6.1	$P < 0.00001$
ACOX	1.0 ± 0.9	16.6 ± 9.2	12.0 ± 5.7	$P < 0.00001$
MTP	1.0 ± 1.0	10.8 ± 3.8	8.8 ± 3.3	$P < 0.00001$
TfR1	1.0 ± 1.1	10.8 ± 11.3	11.8 ± 10.3	$P < 0.00001$
TfR2	1.0 ± 0.4	7.6 ± 3.6	5.6 ± 2.8	$P < 0.00001$
hepcidin	1.0 ± 0.9	11.2 ± 9.6	5.7 ± 3.9	$P < 0.00001$

Note: The value is expressed as folds to mean control values (mean ± S.D.). The deference between the groups was determined using the Kruskal–Wallis test.

Trx, thioredoxin; FATP5, fatty acid transport protein 5; SREBP1c, sterol regulatory element-binding protein 1c; FASN, fatty acid synthase; ACAC, acetyl-coenzyme A carboxylase; PPARα, peroxisome proliferative activated receptor α; CYP2E1, cytochrome P-450 2E1; ACADM, acyl-coenzyme A dehydrogenase; ACOX, acyl-coenzyme A oxidase; MTP, microsomal triglyceride transfer protein; TfR1, transferrin receptor 1; TfR2, transferrin receptor 2.

Table 5 Correlation of the gene levels with liver histology*

	Stage		Grade	
	r	*P* value	*r*	*P* value
Trx	0.209	0.074	0.132	0.266
FATP5	−0.334	0.004	−0.339	0.003
SREBP1c	−0.264	0.024	−0.283	0.015
FASN	−0.158	0.178	−0.182	0.124
ACAC	−0.264	0.024	−0.313	0.007
PPARα	−0.253	0.031	−0.244	0.038
CYP2E1	−0.264	0.024	−0.293	0.012
ACADM	−0.241	0.040	−0.246	0.036
ACOX	−0.213	0.070	−0.213	0.071
MTP	−0.262	0.025	−0.271	0.020
TfR1	0.227	0.037	0.182	0.089
TfR2	−0.307	0.008	−0.318	0.006
hepcidin	−0.251	0.032	−0.221	0.060

*Using Spearman's test. Trx, thioredoxin; FATP5, fatty acid transport protein 5; SREBP1c, sterol regulatory element-binding protein 1c; FASN, fatty acid synthase; ACAC, acetyl-coenzyme A carboxylase; PPARα, peroxisome proliferative activated receptor α; CYP2E1, cytochrome P-450 2E1; ACADM, acyl-coenzyme A dehydrogenase; ACOX, acyl-coenzyme A oxidase; MTP, microsomal triglyceride transfer protein; TfR1, transferrin receptor 1; TfR2, transferrin receptor 2.

did not reach statistical significance (Table 5). In parallel with these findings, the level of hepatic steatosis decreased as the stage and grade progressed (Fig. 1). None of these genes was independently correlated with hepatic steatosis (not shown).

TfR1 and TfR2

The hepatic iron score (HIS) tended to increase as the stage progressed (Table 6). We examined the levels of TfR1 and TfR2, since the uptake of serum iron by hepatocytes is largely through a transferrin-bound form.[16] The levels of both of these genes were significantly higher in the NAFLD patients than in the controls (Table 4). When values were compared between simple steatosis and NASH using the Mann–Whitney's test, the TfR2 level was significantly ($P < 0.01$) higher in the simple steatosis patients than the NASH patients. The TfR1 level significantly increased as the stage progressed, whereas that of TfR2 significantly decreased as the stage and grade progressed (Table 5). Neither TfR1 nor TfR2 were independently correlated with HIS (not shown).

Table 6 Hepatic iron score and the stage

	Hepatic iron score				
	0	1	2	3	4
Stage 0	11	11	3	0	1
Stage 1	7	1	1	1	0
Stage 2	3	4	3	2	0
Stage 3	4	4	2	2	0
Stage 4	0	0	0	0	1

Note: The value represents the number of patients. Simple steatosis was considered as stage "0". $r = 0.213$, $P = 0.099$, iron score vs stage: Spearman's test.

Hepcidin

Hepcidin is known to be secreted from hepatocytes and regulates systemic iron transport.[16] The hepcidin level was significantly different among the controls, the simple steatosis patients and the NASH patients. The value was higher in the simple steatosis patients than in the NASH patients (Table 4). Hepcidin level decreased significantly as the stage progressed (Table 5). Since the ratio of hepcidin to iron load has been reported to evaluate the appropriateness of the hepcidin response to iron overload,[17] we divided hepcidin mRNA levels by serum ferritin levels or HIS. The ratios of hepcidin mRNA/ferritin and hepcidin mNA/HIS were signifi-

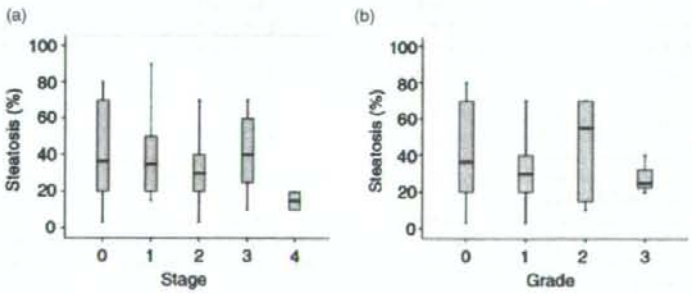

Figure 1 Distributions of the level of hepatic steatosis in association with the stage (a) and grade (b). The level of steatosis decreased as the stage and grade progressed.

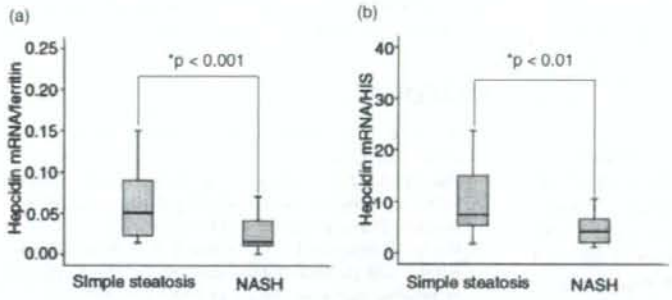

Figure 2 The ratio of hepcidin mRNA levels to serum ferritin levels (a) and that of hepcidin mRNA levels to hepatic iron score (HIS) (b). Hepcidin mRNA levels corrected for iron overload were significantly lower in NASH patients than in simple steatosis patients. *Mann-Whitney U-test.

cantly lower in NASH patients than simple steatosis patients (Fig. 2). The ratio of hepcidin mRNA/ferritin was significantly correlated with stage ($r = -0.523$, $P < 0.00005$) and grade ($r = -0.436$, $P < 0.0005$). The same results were obtained from the ratio of hepcidin mRNA/HIS ($r = -0.424$, $P < 0.01$ vs stage; $r = -0.373$, $P < 0.05$ vs grade). We compared hepcidin mRNA levels with metabolic variables and found that the level of hepcidin was significantly correlated with both total cholesterol ($r = 0.323$, $P < 0.01$) and triglyceride ($r = 0.323$, $P < 0.01$). The ratio of hepcidin mRNA/ferritin was also significantly correlated with total cholesterol ($r = 0.365$, $P < 0.005$).

DISCUSSION

IN THIS STUDY, we investigated the expression levels of hepatic genes that play significant roles in the metabolism of fatty acids and iron. Their roles in hepatocytes include the uptake, synthesis, oxidation, storage and excretion of fatty acids,[10,18,19] the uptake of iron and the regulation of systemic iron transport.[16] We found that the levels of these genes were significantly higher in NAFLD patients than controls. In addition, we found some novel findings. However, none of the individual genes was independently correlated with hepatic steatosis. These results indicated that neither the lack of nor increase in the expression levels of any of these genes plays an independent role in the development of fatty liver.

Insulin resistance is the "first hit" in the development of NASH,[9] which is characterized by an increase in the uptake and synthesis of fatty acids in hepatocytes.[15] Nevertheless, our results showed that the levels of fatty acid-related genes decreased in the later stages despite the presence of insulin resistance. In parallel with these findings, the level of hepatic steatosis also decreased. Considering that fat is the fuel involved in progressive liver injuries,[20] these findings might be associated with "burnout" NASH.[21] Although the underlying reason for this is unclear, some possibilities should be considered. Because hepatic adenosine 5′-triphosphate (ATP) levels tend to be decreased in fatty liver,[22] hepatic adenosine monophosphate-activated protein kinase (AMPK) should be activated.[23] AMPK is known to activate catabolic pathways and switch off protein, carbohydrate and lipid synthesis, such that cellular energy levels remain unchanged.[23] Thus, activated AMPK in hepatocytes might contribute to the decrease in the expression levels of fatty acid-related genes. Anti-diabetic drugs, which ameliorate liver injuries in patients with NASH, have been reported to activate AMPK.[24] Interestingly, the levels of all the genes involved in fatty acid metabolism were lower in the patients treated with insulin sensitizers than in those treated with other agents or followed with diet restriction. Statistical significance was achieved only in FATP5 ($P < 0.05$, Mann–Whitney's test). However, these results may be difficult to evaluate or apply generally, because the numbers of patients were small.

Hepatic iron load has been documented to be another key player in the progression from steatosis to steatohepatitis.[11] Hepatic iron load has been attributed to the Cys282Tyr mutation in the hemochromatosis gene.[11] This mutation decreases hepatic synthesis of hepcidin, resulting in the facilitation of iron absorption from the duodenum.[16] Our results showed that hepatic iron scores tended to correlate with the histological stage of NAFLD. Furthermore, the ratios of hepcidin mRNA/ferritin and hepcidin mRNA/HIS were significantly lower in NASH patients than in simple steatosis patients. This insufficient production of hepcidin may not be attributed to the genetic mutation, since known mutations of hemochromatosis-associated genes have been reported to be rare among Japanese patients.[25]

Interestingly, the hepcidin level was significantly correlated with the levels of total cholesterol and triglycerides. These findings coincide with those recently reported by Barisani *et al.*,[17] who reported that the hepcidin mRNA/ferritin ratio and the hepcidin mRNA/tissue iron score ratio were significantly lower in the NAFLD group with hepatic iron overload than in the NAFLD group without iron overload,[17] and that the level of hepatic hepcidin mRNA was significantly correlated with lipid parameters.[17] Our findings, in concert with those of Barisani *et al.*, suggest that more severe forms of NAFLD are associated with insufficient hepcidin production, and that lipid metabolism might be involved in hepcidin synthesis. Alternatively, the hepatic levels of TfR1 and TfR2 were significantly higher in NAFLD patients than controls. Therefore, TfR1 and TfR2 would be expected to promote hepatic iron load irrespective of iron absorption from the duodenum.

TfR1 is ubiquitously expressed in the human body,[16] while TfR2 is dominantly expressed in specific organs including the liver.[26] TfR1 has a high affinity with transferrin[27] and its expression is regulated by the iron-responsive element (IRE) in the 3′-untranslated regions of mRNAs.[16] In the NAFLD patients, the TfR1 level increased significantly as the stage progressed. Since ROS stabilize TfR1 mRNA via activation of iron regulatory proteins that interact with IRE,[16] hepatic oxidative stress should upregulate TfR1 in NAFLD.

TfR2 was recently identified as a novel transferrin receptor,[26] although the expression mechanisms have not been fully determined.[28] Similarly, neither the physiological nor pathological role of TfR2 in the liver has been documented. The expression level of TfR2 was higher in NAFLD patients than controls. At present, the association between the level of TfR2 and the pathogenesis of NAFLD remains unknown. Regardless of the role of TfR2, we have reported that the TfR2 level is significantly correlated with that of PPARα.[29] It is of much interest to speculate that PPARα might contribute to the regulation of TfR2, since PPARα may be upregulated in NAFLD by intrinsic PPARα ligands. This hypothesis is under investigation in our institute.

In summary, we investigated the metabolism of fatty acids and iron in the livers of NAFLD patients. Steatosis-related metabolism is attenuated as the disease progresses, whereas iron load-related metabolism is exacerbated. Based on these findings, we hypothesize that anti-lipid synthesis should be considered in the early stages and that iron reduction should be considered in the later stages. The former therapies may thus include body weight reduction and insulin-sensitizing drugs, and the latter therapies may include phlebotomy, iron-restriction diets and/or antioxidants.

REFERENCES

1 Angulo P. Nonalcoholic fatty liver disease. *N Engl J Med* 2002; **346**: 1221–31.
2 Hui JM, Kench JG, Chitturi S *et al.* Long-term outcomes of cirrhosis in nonalcoholic steatohepatitis compared eith hepatitis C. *Hepatology* 2003; **38**: 420–7.
3 Ratziu V, Bonyhay L, Di Martino V *et al.* Survival, liver failure, and hepatocellular carcinoma in obesity-related cryptogenic cirrhosis. *Hepatology* 2002; **35**: 1485–93.
4 Suzuki A, Lindor K, St Saver J *et al.* Effect of changes on body weight and lifestyle in nonalcoholic fatty liver disease. *J Hepatol* 2005; **43**: 1060–6.
5 Marchesini G, Brizi M, Bianchi G, Tomassetti S, Zoli M, Melchionda N. Metformin in non-alcoholic steatohepatitis. *Lancet* 2001; **358**: 893–4.
6 Abdelmalek MF, Angulo P, Jorgensen RA, Sylvestre PB, Lindor KD. Betaine, a promising new agent for patients with nonalcoholic steatohepatitis: results of a pilot study. *Am J Gastroenterol* 2001; **96**: 2711–7.
7 Facchini FS, Hua NW, Stoohs RA. Effect of iron depletion in carbohydrate-intolerant patients with clinical evidence of nonalcoholic fatty liver disease. *Gastroenterology* 2002; **122**: 931–9.
8 Lindor KD, Kowdley KV, Heathcote EJ *et al.* Ursodeoxycholic acid for treatment of nonalcoholic steatohepatitis: results of a randomized trial. *Hepatology* 2004; **39**: 770–8.
9 Day CP, James OF. Steatohepatitis: a tale of two "hits"? *Gastroenterology* 1998; **114**: 842–5.
10 Browning JD, Horton JD. Molecular mediators of hepatic steatosis and liver injury. *J Clin Invest* 2004; **114**: 147–52.
11 George DK, Goldwurm S, MacDonald GA *et al.* Increased hepatic iron concentration in nonalcoholic steatohepatitis is associated with increased fibrosis. *Gastroenterology* 1998; **114**: 311–8.
12 Brunt EM, Janney CG, Di Bisceglie AM, Neuschwander-Tetri BA, Bacon BR. Nonalcoholic steatohepatitis: a proposal for grading and staging the histological lesions. *Am J Gastroenterol* 1999; **94**: 2467–74.
13 Searle J, Kerr JFR, Halliday JW, Powell LW. Iron storage disease. In: MacSween RNM, Anthony PP, Scheuer PJ, eds. *Pathology of the Liver*, 3rd edn. London: Churchill Livingstone, 1994; 219–41.
14 Hirota K, Nakamura H, Masutani H, Yodoi J. Thioredoxin superfamily and thioredoxin-inducing agents. *Ann N Y Acad Sci* 2002; **957**: 189–99.
15 Sumida Y, Nakashima T, Yoh T *et al.* Serum thioredoxin levels as a predictor of steatohepatitis in patients with non-alcoholic fatty liver disease. *J Hepatol* 2003; **38**: 32–8.
16 Hentze MW, Muckenthaler MU, Andrews NC. Balancing acts: molecular control of mammalian iron metabolism. *Cell* 2004; **117**: 285–97.

17 Barisani D, Pelucchi S, Mariani R *et al.* Hepcidin and iron-related gene expression in subjects with Dysmetabolic Hepatic Iron Overload. *J Hepatol* 2008; **49**: 123–33.
18 Doege H, Baillie RA, Ortegon AM *et al.* Targeted deletion of FATP5 reveals multiple functions in liver metabolism: alterations in hepatic lipid homeostasis. *Gastroenterology* 2006; **130**: 1245–58.
19 Goldberg IJ, Ginsberg HN. Ins and outs modulating hepatic triglyceride and development of nonalcoholic fatty liver disease. *Gastroenterology* 2006; **130**: 1343–6.
20 Day CP, James OF. Hepatic steatosis: innocent bystander or guilty party? *Hepatology* 1998; **27**: 1463–6.
21 Caldwell SH, Oelsner DH, Iezzoni JC, Hespenheide EE, Battle EH, Driscoll CJ. Cryptogenic cirrhosis: clinical characterization and risk factors for underlying disease. *Hepatology* 1999; **29**: 664–9.
22 Chavin KD, Yang S, Lin HZ *et al.* Obesity induces expression of uncoupling protein-2 in hepatocytes and promotes liver ATP depletion. *J Biol Chem* 1999; **274**: 5692–700.
23 Hardie DG, Scott JW, Pan DA, Hudson ER. Management of cellular energy by the AMP-activated protein kinase system. *FEBS Lett* 2003; **546**: 113–20.
24 Fryer LG, Parbu-Patel A, Carling D. The anti-diabetic drugs rosiglitazone and metformin stimulate AMPK-activated protein kinase through distinct signaling pathways. *J Biol Chem* 2002; **277**: 25226–32.
25 Yamauchi N, Itoh Y, Tanaka Y *et al.* Clinical characteristics and prevalence of GB virus C, SEN virus, and HFE gene mutation in Japanese patients with nonalcoholic steatohepatitis. *J Gastroenterol* 2004; **39**: 654–60.
26 Kawabata H, Yang R, Hirama T *et al.* Molecular cloning of transferring receptor 2. *J Biol Chem* 1999; **274**: 20826–32.
27 Robb AD, Ericsson M, Wessling-Resnick M. Transferrin receptor 2 mediates a biphasic pattern of transferrin uptake associated with ligand delivery to multivesicular bodies. *Am J Physiol Cell Physiol* 2004; **287**: 1769–75.
28 Kawabata H, Germain RS, Ikezoe T *et al.* Regulation of expression of murine transferrin receptor 2. *Blood* 2001; **98**: 1949–54.
29 Mitsuyoshi H, Yasui K, Harano Y, Itoh Y, Okanoue T. Analysis of hepatic expression of genes involved in lipid and iron metabolism in nonalcoholic fatty liver disease. *Hepatology* 2007; **46**: 733A.

Journal of Medical Virology 80:1354–1362 (2008)

Substitution of Amino Acid 70 in the Hepatitis C Virus Core Region of Genotype 1b Is an Important Predictor of Elevated Alpha-Fetoprotein in Patients Without Hepatocellular Carcinoma

Norio Akuta,[1]* Fumitaka Suzuki,[1] Yusuke Kawamura,[1] Hiromi Yatsuji,[1] Hitomi Sezaki,[1] Yoshiyuki Suzuki,[1] Tetsuya Hosaka,[1] Masahiro Kobayashi,[1] Mariko Kobayashi,[2] Yasuji Arase,[1] Kenji Ikeda,[1] and Hiromitsu Kumada[1]

[1]Department of Hepatology, Toranomon Hospital, Tokyo, Japan
[2]Liver Research Laboratory, Toranomon Hospital, Tokyo, Japan

Previous studies identified amino acid (aa) substitutions of the hepatitis C virus core region of genotype 1b (HCV-1b core region) and elevated serum alpha-fetoprotein (AFP) levels as predictors of poor virologic response to pegylated interferon (PEG-IFN) plus ribavirin (RBV), and also as risk factors for hepatocarcinogenesis. The present study evaluated the impact of aa substitutions of HCV-1b core region on AFP, as a surrogate marker of hepatocarcinogenesis, on AFP levels in 569 Japanese patients with HCV-1b but without HCC, and investigated the predictive factors of elevated AFP ($\geq$11 μg/L). High AFP levels were detected in 27.4% of the patients. The rate of hepatocarcinogenesis in a group of 109 patients who received IFN monotherapy and followed-up for 15 years, was significantly higher in patients with abnormal than normal AFP. Multivariate analysis of 569 patients identified fibrosis stage (*F*3,4), aspartate aminotransferase ($\geq$76 IU/L), substitution of aa 70 (glutamine or histidine), and platelet count ($<15.0 \times 10^4$/μl) as significant determinants of elevated AFP. In 49 patients with abnormal AFP levels and substitutions at aa 70 who were treated with PEG-IFN + RBV, the rate of normalization of AFP was significantly lower in non-virological responders (28.6%) than in transient (71.4%) and sustained (100%) virological responders. The results indicated that substitution of aa 70 of HCV-1b core region is an important predictor of elevated AFP in non-HCC patients, and that eradication of the mutant virus normalizes AFP. The results highlight the importance of eradication of mutant type virus of aa 70 for reducing the risk of hepatocarcinogenesis.
J. Med. Virol. 80:1354–1362, 2008.

KEY WORDS: HCV; core region; genotype; AFP; hepatocellular carcinoma; glutamine; histidine

INTRODUCTION

Hepatitis C virus (HCV) usually causes chronic infection that can result in chronic hepatitis, liver cirrhosis, and hepatocellular carcinoma (HCC) [Dusheiko, 1998; Ikeda et al., 1998; Niederau et al., 1998; Kenny-Walsh, 1999; Akuta et al., 2001]. In patients with HCV-chronic hepatitis, treatment with interferon (IFN) can induce viral clearance and marked biochemical and histological improvement [Davis et al., 1989; Di Bisceglie et al., 1989]. Especially, pegylated interferon (PEG-IFN) plus ribavirin (RBV) combination therapy can achieve a high sustained virological response, although patients with non-virological response who remain HCV-RNA-positive at the completion of treatment are also encountered [Akuta et al., 2005, 2006, 2007a,b,c]. Previous studies indicated that amino acid (aa) substitutions at position 70 and/or 91 in the HCV core region of genotype 1b (HCV-1b core region) and elevated alpha-fetoprotein (AFP) levels were predictors of poor virological response to PEG-IFN plus RBV therapy [Akuta et al., 2005, 2006, 2007a,b,c; Donlin et al., 2007], and also risk factors and surrogate markers of hepatocarcinogenesis [Ikeda et al., 2006; Akuta et al., 2007d].

*Correspondence to: Norio Akuta, MD, Department of Hepatology, Toranomon Hospital, 2-2-2 Toranomon, Minato-ku, Tokyo 105-0001, Japan. E-mail: akuta-gi@umin.ac.jp

Accepted 11 March 2008
DOI 10.1002/jmv.21202
Published online in Wiley InterScience (www.interscience.wiley.com)

The use of elevated AFP as a predictor of early hepatocarcinogenesis in non-HCC patients might be clinically useful. AFP is a fetal glycoprotein produced by the yolk sac and fetal liver [Bergstrand and Czar, 1956], and has been used widely as a serum marker for the diagnosis of HCC [Sato et al., 1993; Johnson, 2001]. Furthermore, elevated serum AFP is also associated with various chronic liver diseases and hepatic regeneration [Kew et al., 1973; Silver et al., 1974; Elftherious et al., 1977; Alpert and Feller, 1978]. Although a mild rise in serum AFP is commonly seen in chronic HCV-infected patients, its clinicopathological significance remains to be defined. Previous studies indicated that high serum AFP levels correlated with fibrosis stages 3 and 4 [Bayati et al., 1998; Chu et al., 2001; Hu et al., 2002, 2004], levels of aspartate aminotransferase (AST) and alanine aminotransferase (ALT) [Chu et al., 2001; Stein and Myaing, 2002; Hu et al., 2004], prothrombin time [Hu et al., 2004], and HCV-1b [Chu et al., 2001], in chronic HCV-infected patients. However, it is not clear whether mild elevation of AFP in the absence of HCC is associated with eventual development of HCC in HCV-infected patients. Furthermore, the impact of viral factors, such as aa substitutions of HCV-1b core region, on elevated AFP is still unclear.

The aims of the present study conducted in HCC-free Japanese patients infected with HCV-1b, were the following. (1) To evaluate the impact of elevated AFP, especially mild elevation of AFP, on hepatocarcinogenesis in IFN-treated patients without HCC during a long-term (15 years) follow-up period. (2) To identify the impact of aa substitutions in the core region on AFP levels in such patients, and determine the predictive factors for elevated AFP. (3) To investigate the normalization rates of AFP levels after eradication of HCV-RNA by PEG-IFN plus RBV combination therapy.

PATIENTS AND METHODS

Study Population

At Toranomon Hospital, Tokyo, Japan, 2,841 HCV-infected Japanese patients were recruited consecutively into the study protocol of IFN monotherapy between February 1987 and August 2007, and 929 HCV-infected Japanese patients were consecutively recruited into the study protocol of the combination therapy with PEG-IFNα-2b plus RBV between December 2001 and August 2007. Among these, 569 patients were selected in the present retrospective study based on the following criteria. (1) They were negative for hepatitis B surface antigen (radioimmunoassay, Dainabot, Tokyo), positive for anti-HCV (third-generation enzyme immunoassay, Chiron Corp., Emerville, CA), and positive for HCV-RNA qualitative analysis with PCR (nested PCR or Amplicor™, Roche Diagnostics, Indianapolis, IN). (2) They were naive to antiviral treatment. (3) They were infected with HCV-1b alone. (4) AFP levels were measured frequently, and substitutions of aa 70 or 91 in the HCV core region (HCV mutant-70 and HCV mutant-91, respectively) were determined at the commencement of the first course of antiviral treatment. (5) They were free of HCC based on clinical examination, laboratory tests, and imaging studies at baseline. (6) None was an alcoholic; lifetime cumulative alcohol intake was <500 kg (mild to moderate alcohol intake). (7) All were free of coinfection with human immunodeficiency virus. (8) None had other forms of hepatitis, such as hemochromatosis, Wilson disease, primary biliary cirrhosis, alcoholic liver disease, and autoimmune liver disease. (9) Each signed a consent form of the study protocol that had been approved by the Human Ethics Review Committee of Toranomon Hospital. Table I summarizes the profiles and laboratory data of the 569 patients at the commencement of antiviral treatment. They included 347 males and 222 females, aged 18–77 years (median, 55 years). Of the total group of 569 patients, 229 received IFN monotherapy, while 340 were treated with PEG-IFN plus RBV combination therapy. Among the patients who received IFN monotherapy, 109 patients started the monotherapy between February 1987 and August 1992, received at least two courses of such therapy, and were followed-up for 15 years. They were evaluated for the rate of development of HCC, associated with a rise in AFP level relative to that measured before the first course IFN monotherapy (baseline). At baseline, the latter group consisted of 80 males and 29 females, aged 22–69 with a median age of 46 years. The numbers of patients with fibrosis stages 1, 2, 3, and 4 were 57, 37, 14, and 1, respectively. The median AST and ALT levels were 85 IU/L (range, 27–400 IU/L) and 138 IU/L (range, 50–594 IU/L), respectively. The median platelet count was $17.0 \times 10^4/\mu l$ (range, 9.8×10^4 to $31.2 \times 10^4/\mu l$). The median viremia level was 5.8 Mequiv./ml (range, <0.5–46.5 Mequiv./ml). The median AFP level was 5 μg/L (range, 2–239 μg/L). The median follow-up time was 16.0 years (range, 0.1–20.3 years). With regard to

TABLE I. Profile and Laboratory Data of 569 Patients Infected with HCV Genotype 1b

Number of patients	569
Sex (male/female)	347/222
Age (years)*	55 (18–77)
Serum aspartate aminotransferase (IU/L)*	59 (17–400)
Serum alanine aminotransferase (IU/L)*	84 (15–594)
Platelet count ($\times 10^4/\mu l$)*	16.1 (3.8–40.2)
Serum alpha-fetoprotein (μg/L)*	6 (2–459)
Fibrosis stage (F1/F2/F3/F4/ND)	227/132/76/17/117
Level of viremia (high titer/low titer)**	522/47
Amino acid substitutions in core region***	
aa 70 (wild/mutant)	340/229
aa 91 (wild/mutant)	341/228
Treatment	
IFN monotherapy/PEG-IFN plus RBV	229/340

Data are number of patients, except those denoted by *, which represent the median (range) values. (**) Level of viremia was evaluated as high titer (≥1.0 Meq/ml, or ≥100 KIU/ml) and low titer (<1.0 Meq/ml, or <100 KIU/ml). (***) The presence of arginine at aa 70 was evaluated as wild type, while other patterns (glutamine/histidine) as mutant type. The presence of leucine at aa 91 was evaluated as wild type, while other patterns (methionine) as mutant type.
Normal reference ranges: 11–38 IU/L for aspartate aminotransferase; 6–50 IU/L for alanine aminotransferase (IU/L); ≤10 μg/L for alpha-fetoprotein. ND: not done; IFN: interferon; PEG-IFN: pegylated interferon; RBV: ribavirin.

the protocol of IFN monotherapy, 68 (62.4%) patients received IFN-α alone; 36 (33.0%) patients received IFN-β alone; while the remaining 5 (4.6%) patients received a combination of IFN-α and IFN-β. The median IFN dose per day of 6 million units (MU, range; 1–10 MU) was administered. IFN monotherapy included initial aggressive induction therapy, consisting of every day within the first 8 weeks of commencement of therapy, followed subsequently by three times per week.

On the other hand, 340 patients received PEG-IFNα-2b combination therapy at a median dose of 1.5 μg/kg (range, 0.8–1.8 μg/kg) subcutaneously each week plus oral RBV at a median dose of 11.0 mg/kg (range, 3.4–14.2 mg/kg) daily for a median duration of 48 weeks (range, 9–112 weeks).

In this study, patients who were HCV-RNA-negative by qualitative PCR analysis at 24 weeks after the completion of therapy, were defined as sustained virological responders. On the other hand, patients who were HCV-RNA-negative by qualitative PCR analysis at the completion of 24-week treatment but became HCV-RNA-positive after the 24-week therapy, were defined as transient virological responders. Patients who remained HCV-RNA-positive by quantitative and/or qualitative PCR analyses at the completion and after treatment, were defined as non-virological responders.

Laboratory Investigations

Blood samples were obtained at least once every month before, during, and after treatment, and were analyzed for AST, ALT, and HCV-RNA levels. The serum samples were frozen at −80°C within 4 hr of collection and then thawed at the time of measurement. HCV genotype was determined by PCR using a mixed primer set derived from nucleotide sequences of NS5 region [Chayama et al., 1993]. HCV-RNA levels were measured by branched DNA assay version 2.0 (Chiron Corp., Emeryville, CA) or quantitative PCR assay (Cobas Amplicor HCV monitor v 2.0 using the 10-fold dilution method, Roche) before, during, and after the antiviral therapy. The lower limits of these assays were 0.5 Meq/ml (10^6 genomic equivalents per milliliter) by branched DNA assay, or 5 KIU/ml by quantitative PCR assay. Samples with undetectable levels by these quantitative assays (<0.5 Meq/ml, or <5 KIU/ml) were checked also by HCV-RNA qualitative analysis with PCR (nested PCR or Amplicor™, Roche) during and after treatment especially, and the results were expressed as positive or negative. The lower limit of the assay was 50 IU/ml. In this study, levels of viremia were evaluated as high titer (≥1.0 Meq/ml, or ≥100 KIU/ml) and low titer (<1.0 Meq/ml, or <100 KIU/ml).

Histopathological Examination of Liver Biopsies

Liver biopsy specimens were obtained percutaneously or at peritoneoscopy using a modified Vim Silverman needle with an internal diameter of 2 mm (Tohoku University style, Kakinuma Factory, Tokyo). The biopsy material was fixed in 10% formalin, and stained with hematoxylin and eosin, Masson's trichrome, silver impregnation, and periodic acid–Schiff after diastase digestion. All specimens for examination contained six or more portal areas. Histopathological diagnosis was confirmed by an experienced liver pathologist (H.K.) who was blinded to the clinical data. Chronic hepatitis and liver cirrhosis were diagnosed based on histological assessment according to the scoring system of Desmet et al. [1994].

Detection of Amino Acid Substitutions in Core Region

Okamoto et al. [2007] developed a simple PCR method for detecting substitutions of aa 70 or aa 91 in HCV-1b core region using mutation-specific primer, as an alternative to the direct sequencing method. The major protein type was determined based on the relative intensity of the bands for wild (aa 70: arginine, aa 91: leucine) and mutant HCV-1b (aa 70: glutamine/histidine, aa 91: methionine) in agarose gel electrophoresis. If the intensities of the bands were similar, the case was regarded as competitive. The detection rate was 94.4%, the sensitivity was 10 KIU/ml using quantitative assay with PCR (Cobas Amplicor HCV monitor v 2.0 using the 10-fold dilution method, Roche), the reproducibility was high, and consistency with direct sequencing was 97.1% in positive cases. Mutation in this study refers to substitution from consensus sequence. In previous studies, HCV-J (accession no. D90208) was considered a prototype and the aa substitution was evaluated by comparison with the consensus sequence prepared from 50 clinical trial samples [Kato et al., 1990; Akuta et al., 2005]. In the present study, PCR using primers specific for substitutions of aa 70 or aa 91 was performed in samples collected from 454 patients [Okamoto et al., 2007]; the remaining 115 patients were analyzed by direct sequencing [Akuta et al., 2005, 2006].

Diagnosis of Hepatocellular Carcinoma

Patients were examined for HCC by abdominal ultrasonography every 3–6 months. If HCC was suspected based on ultrasonographic results, additional procedures, such as computed tomography, magnetic resonance imaging, abdominal angiography, and ultrasonography-guided tumor biopsy, were used to confirm the diagnosis.

Statistical Analysis

Non-parametric tests were used to compare variables between groups, including the Mann–Whitney *U*-test, chi-squared test and Fisher's exact probability test. Multiple comparisons were conducted by the Bonferroni test. The cumulative rate of hepatocarcinogenesis was calculated using the Kaplan–Meier technique; differences between carcinogenesis curves between groups were tested using the log-rank test. Statistical analyses of the rate of hepatocarcinogenesis according to

groups were calculated using the period from start of the first course of IFN monotherapy. Univariate and multivariate logistic regression analyses were used to determine the independent predictive factors of elevated AFP. The odds ratios and 95% confidence intervals (95% CI) were also calculated. All P values less than 0.05 by the two-tailed test were considered significant. Variables that achieved statistical significance ($P < 0.05$) or marginal significance ($P < 0.10$) on univariate analysis were entered into multiple logistic regression analysis to identify significant independent factors. Potential predictive factors associated with elevated AFP included the following pretreatment variables: sex, age, AST, ALT, platelets, pathological staging, viremia level, and aa substitutions in the core region. Statistical analyses were performed using the SPSS software (SPSS Inc., Chicago, IL).

RESULTS

Cumulative Rate of Hepatocarcinogenesis According to AFP Levels

Of the 229 patients who received IFN monotherapy, 109 could be evaluated for the rate of development of HCC based on AFP levels measured at the start of the first course IFN monotherapy (baseline), during a follow-up period of 15 years. All 109 patients received two or more courses of IFN monotherapy; 66 patients received two courses of IFN (including 16 patients who achieved sustained virological response), 35 patients received three courses (including 4 patients who achieved sustained virological response), 7 patients received four courses (including 1 patient who achieved sustained virological response), and one patient received six courses (did not achieve sustained virological response). Thus, 21 of 109 patients achieved sustained virological response after multicourses of IFN monotherapy. For those who received 1, 2, 3, 4, 5, and 6 courses of IFN monotherapy, the median total duration of IFN therapy was 23.9 weeks (range, 0.9–134.7 weeks), 24.0 (range, 1.3–313.7), 25.1 (range, 3.1–193.1), 40.3 (range, 21.0–86.3), 23.6, and 67.9, respectively, and the median total dose of IFN was 526 MU (range, 22–1393 MU), 589 (range, 57–4005), 501 (range, 28–3477), 536 (range, 363–1553), 708, and 1200, respectively. The median cumulative total duration and cumulative total dose, which represented the cumulative total duration and total dose of every course of every patient were 57.7 weeks (range, 14.0–467.6 weeks) and 1380 MU (range, 521–4805 MU), respectively. The median period during which no IFN was administered was 3.7 years (range, 0.1–7.0 years). Finally, the median dose of IFN per week was 22.5 MU (range, 3.7–43.9).

During the follow-up, 8.6% (7 of 81 patients), 20.0% (3 of 15), and 38.5% (5 of 13) developed HCC in patients with AFP levels below 1 (≤10 μg/L), from 1 to 2 (11–20 μg/L), and above twice (≥21 μg/L) the upper limit of normal (ULN), respectively. In patients with AFP levels below 1, from 1 to 2, and above 2 times the ULN, the cumulative hepatocarcinogenesis rates were 0, 7.1, 0% at the end of 5 years; 3.1, 23.4, 37.5% at the end of 10 years; and 14.5, 23.4, 58.3% at the end of 15 years, respectively. The rates were significantly different among the three groups ($P < 0.001$; log-rank test) (Fig. 1). Especially, the rate of hepatocarcinogenesis in patients with normal AFP levels was significantly lower than in those with AFP levels above twice ULN ($P < 0.001$), and tended to be lower than in those with AFP levels from 1 to 2 times ULN ($P = 0.070$). The rate of hepatocarcinogenesis in patients with AFP levels above twice ULN was not significantly higher than in those with AFP levels from 1 to 2 times ULN. Thus, the rate of hepatocarcinogenesis was significantly higher in patients with abnormal AFP levels than in those with normal AFP levels ($P < 0.001$).

Predictive Factors of Elevated AFP in Univariate and Multivariate Analyses

The virological, clinical, and biochemical features of the whole population sample of 569 patients were analyzed to determine factors that could predict elevated AFP (≥11 μg/L). Elevated AFP was detected in 156 of 569 (27.4%) patients. Univariate analysis identified seven parameters that influenced significantly high AFP level. These included age (≥45 years, $P = 0.001$), AST (≥76 IU/L, $P < 0.001$), ALT (≥100 IU/L, $P < 0.001$), platelets ($<15.0 \times 10^4$/μl, $P < 0.001$), stage of fibrosis ($F3,4$, $P < 0.001$), and aa substitutions of the core region (mutant type of aa 70, $P < 0.001$, and aa 91, $P = 0.035$). Multivariate analysis identified four parameters that independently influenced high AFP level, including stage of fibrosis ($F3,4$, $P < 0.001$), AST (≥76 IU/L, $P < 0.001$), substitution of aa 70 (mutant type, $P < 0.001$), and platelet count ($<15.0 \times 10^4$/μl, $P = 0.019$) (Table IIA).

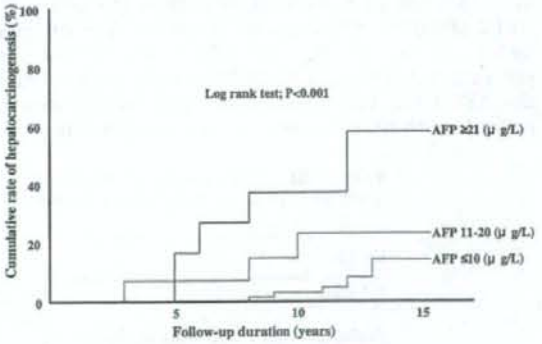

Fig. 1. Cumulative rate of hepatocarcinogenesis according to AFP levels at the start of first course IFN monotherapy. The rate of hepatocarcinogenesis in patients with normal AFP levels (≤10 μg/L) was significantly lower than in those with AFP levels above twice the upper limit of normal (≥21 μg/L) ($P < 0.001$), and tended to be lower than in those with AFP levels from 1 to 2 times the upper limit of normal (11–20 μg/L) ($P = 0.070$). The rate of hepatocarcinogenesis in patients with abnormal AFP levels (≥11 μg/L) was significantly higher than in those with normal AFP levels ($P < 0.001$).